Multiple Scattering approach to X-Ray Absorption Spectroscopy

M. Benfatto

Laboratori Nazionali di Frascati dell'INFN – Frascati ITALY

Plan of these lessons

- **MS Theory**

  Generalities

  Muffin-Tin approximation

  Problems and prospectives

- **XAS spectroscopy**

  Examples

- **Quantitative analysis of the XANES energy region**

  Method and examples

MS Theory

- **It is a method to solve the Sch. Equation in real space -** It has been developed by K. H. Johnson since ’60-’70

$$\left[-\nabla^2 + V(\vec{r})\right]\Psi(\vec{r}) = E\Psi(\vec{r})$$

$$V(\vec{r}) = V_c(\vec{r}) + V_{exc}(\vec{r})$$

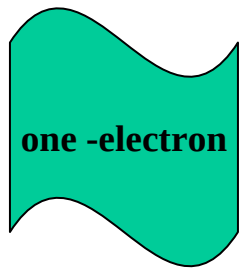

$$V_c(\vec{r}) = \sum_j V^j(\vec{r} - R_j)$$

$$V_{exc}(\vec{r}) = -6\alpha\left[\frac{3}{8\pi}\rho(\vec{r})\right]^{1/3}$$

$$V_c(\vec{r}) = \sum_j V^j(\vec{r} - R_j)$$

Sum of free atom potential ⟷ cluster of atoms

Muffin-Tin approximation

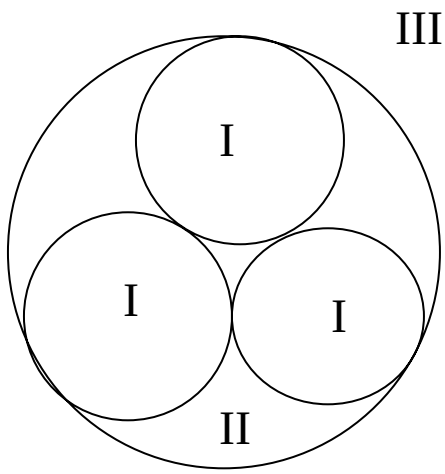

The space is divided in three regions

I region

$$V_I(\vec{r}) = \sum_L V_L(r) Y_L(\hat{r}) \,;\, L \equiv l,m$$

Only the L=0 is considered

II region

$$V_{II}(\vec{r}) = V_{MT} = \frac{1}{\Omega_{II}} \int_{\Omega_{II}} V(\vec{r})\, d\vec{r}$$

V_{MT} is a constant value
The average is over the interstial volume

III region

V_{III} is a spherical average respect respect to the atomic cluster center
It depends to the physical problem to be solved.

We must solve the Sch. equation with this potential

The total w.f. can be expressed as:

$$\Psi = \sum_i \Psi_I + \Psi_{II} + \Psi_{III}$$

- In each atomic region (region I) the w.f. is developed into spherical harmonics:

$$\Psi_I^J(\vec{r}) = \sum_L B_L^J R_l^J(E;r) Y_{lm}(\hat{r})$$

- We impose the continuity of this w.f. and its first derivate with the w.f.in region II V_{MT} is constant $\longrightarrow \Psi_{II}$ is a combination of Bessel and Neumann functions

Compatibility equations between B_L^j coefficients

i) Eigen-values of the bounded molecular states
ii) w.f. in the various regions
iii) Spectroscopies quantities

The outer sphere (regionIII) w.f. determines the type of solution – expression valid for both continuum and bound states problem

$$\Psi_{III} = \sum_{L,L'} [A_L^{III} f_l^{III}(kr_0)\delta_{LL'} + B_{LL'}^{III} g_{l'}^{III}(kr_0)] Y_{L'}(\hat{r}_0)$$

regular part

irregular part

center of the whole molecules

Bound states → Set of homogeneous equation

Molecular energies are the zero of the determinat

MnO_4^- T_d symmetry

Keith H. Johnson

TABLE I

SCF–Xα Electronic Energy Levels (in Rydbergs) of an MnO_4^- Cluster in a Crystalline Environment[a]

Symmetry	Energy Levels
$7a_1$	−0.006
$8t_2$	−0.020
$7t_2$	−0.350
$2e$	−0.526
$1t_1$	−0.682
$6t_2$	−0.761
$6a_1$	−0.775
$1e$	−0.901
$5t_2$	−0.915
$4t_2$ (O $2s$)	−1.785 (−1.732)
$5a_1$ (O $2s$)	−1.813 (−1.732)
$3t_2$ (Mn $3p$)	−4.259 (−3.952)
$4a_1$ (Mn $3s$)	−6.435 (−6.126)
$2t_2$ (O $1s$)	−37.738 (−37.822)
$3a_1$ (O $1s$)	−37.738 (−37.822)
$1t_2$ (Mn $2p$)	−46.513 (−46.274)
$2a_1$ (Mn $2s$)	−54.105 (−53.859)
$1a_1$ (Mn $1s$)	−468.584 (−468.203)

[a] Levels below the dashed line are fully occupied in the ground state; those above the line are empty. Corresponding "free-atom" energy levels are shown in parentheses.

Empty levels

Core states

TABLE IV

Theoretical and Experimental Optical Transition Energies (in eV) for MnO_4^-

Transition	Unrelaxed SCF calculation	Transition-state calculation	Experiment[a]
$1t_1 \rightarrow 2e$	2.1	2.3	2.3
$6t_2 \rightarrow 2e$	3.2	3.3	3.5
$1t_1 \rightarrow 7t_2$	4.5	4.7	4.0
$5t_2 \rightarrow 2e$	5.3	5.3	5.5

[a] See Holt and Ballhausen (1967).

Absorption coefficient from core levels

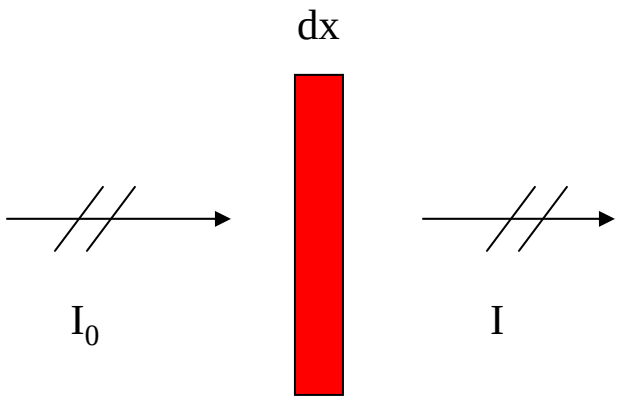

$$dI=\mu(E)\, I\, dx \longrightarrow I=I_0 e^{-\mu(E)x}$$

$$\mu(E) = n_{ab}\, \sigma(E)$$

E is in the X-ray energy range

Density of absorption medium

Photoabsorption cross section

There are other scattering processes
with and without energy loss

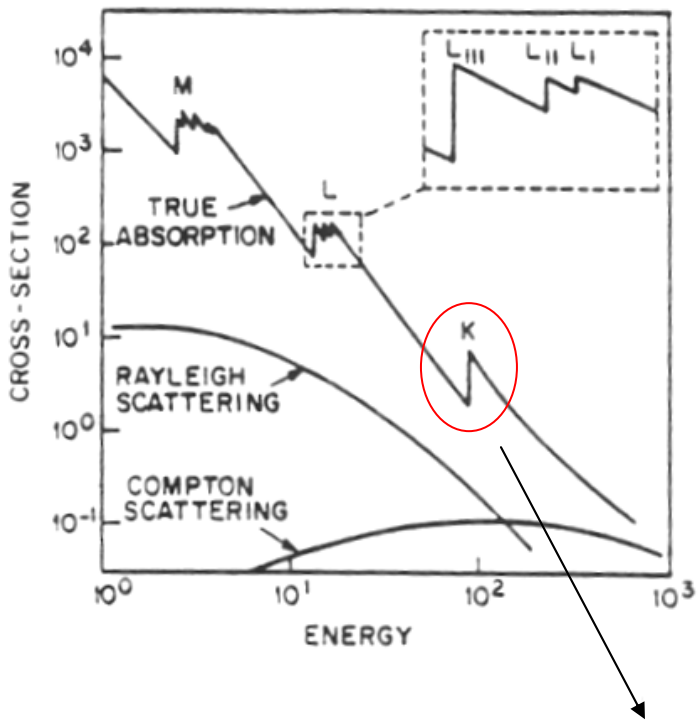

iodine

33 KeV

The photoabsorption process dominates

$K = 1s \longrightarrow \varepsilon p$; $L_I = 2s \longrightarrow \varepsilon p$ .....

Every atomic species has a well defined edges
It is possible to select the species and its environment

Structural and electronic information on the absorbing site from the strong oscillations with energy ⟶ XAFS

Physical process: excitation of core-level electron to continuum states

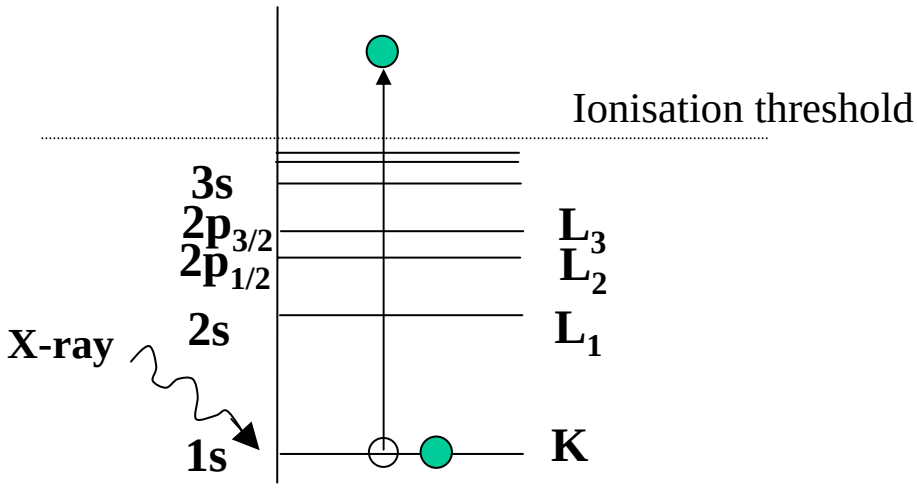

We use the Fermi “golden rule” to calculate the total cross-section of this process

The photoabsorption cross section is defined through the Fermi “golden rule”

$$\sigma(\omega) = 4\pi^2 \alpha\, \omega \sum_f \left| \left\langle \psi_f \left| \vec{\varepsilon} \cdot \vec{r} \right| \psi_c \right\rangle \right|^2 \delta(\omega - E_f + E_c)$$

$$\alpha = \frac{1}{137}$$ Fine structure constant

Dipole approximation $\longleftrightarrow$ $\dfrac{\sigma_q(\omega)}{\sigma_d(\omega)} \approx \dfrac{1}{100}$

ψ_f $\longrightarrow$ continuum part of the w.f.

ψ_c $\longrightarrow$ core w.f. spatially localized

MS approach

- the potential in the extra molecular region III is constant and equal to the muffin-tin potential V_{MT}

- there is not any difference between the regions II and III.

- the external region part of the total wave function can be calculated imposing the T-matrix normalization
- one can treat on the some footing bound states and continuum resonances

“extended continuum” scheme

We can calibrate on the same energy scale the bound state features relative to the continuum features without the need to perform ionization energy calculation

$$\Psi_{III,\underline{L}} = j_{\underline{l}}\ Y_{\underline{L}} + i\sum_{i,L'} B^{i}_{L'}(\underline{L})\,(j_{l'} + i\,n_{l'})\ Y_{L'}$$

Each partial $\underline{L}$ component of the Ψ_{III}

unique energy scale of the pre-edge energy region with the rest of the XAS spectrum.

In this case the amplitude coefficients satisfy

$$B^{i}_{L}(\underline{L}) - t^{i}_{l} \sum_{j \neq i} G^{ij}_{LL'} B^{j}_{L'}(\underline{L}) = t^{i}_{l} J^{io}_{L\underline{L}}$$

where $\longrightarrow$ $t_l = 1/k\, e^{i\delta_l} \sin\delta_l$

$$G^{ij}_{LL'} = 4\pi i \sum_{L''} i^{l''+l-l'} C^{L'}_{LL''} h^{+}_{l''}(kR_{ij}) Y_{L''}(\hat{R}_{ij})$$

Free propagator between site i and j

$G^{ii}_{LL'} \equiv 0$

Gaunt coefficient

$J^{i0}_{L\underline{L}}$

Exciting wave referred to site i

The amplitude at each atomic site i is formed by the one coming from the center plus all arriving from the other sites.

The model is a multiple scattering model for several centers with free propagation in the interstitial region

The previous eq. can be written as:

$$(I - T_a G)\,\vec{B}(\underline{L}) = T_a\,\vec{J}(\underline{L})$$

$$T_a = \delta_{ij}\delta_{LL'}\,t_l^i$$

We need the scattering wave function at site I_0 because of the localization of the core w.f.

$$\sigma(\omega) = A(\omega) \sum_{\underline{L},L,m_\gamma,m_0} \left|B_L^0(\underline{L})\right|^2 \left|(R_L^0(\vec{r}_0) \,|\, r_0 Y_{lm_\gamma}(\hat{r}_0) \,|\, \phi_{l_0}(r_0) Y_{L_0}(\hat{r}_0))\right|^2$$

$$A(\omega) = 2\pi\alpha\omega(4\pi/3)^2\frac{k}{\pi}$$

$$\begin{cases} k = \sqrt{E} \\ E = \omega - I_0 \end{cases}$$

unpolarized photoabsorption cross section

Energies k^2 are measured in Rydbergs (1 Ry = 13.60529 eV) and lengths in Bohrs.

Optical theorem

$$\sum_{\underline{L}} [B^0_L(\underline{L})]^* [B^0_{L'}(\underline{L})] = \mathrm{Im}[(I - T_a G)^{-1} T_a]^{00}_{LL'}$$

$$\tau^{00}_{LL'} = [(I - T_a G)^{-1} T_a]^{00}_{LL'}$$

$$\begin{pmatrix} .. & & G_{ij} \\ & (t^i_\ell)^{-1} & \\ G_{ji} & & .. \end{pmatrix}^{-1}$$

scattering path operator – it contains all the structural and electronic information

complete equivalence between band structure, Green function and MS approach

Photoabsorption cross section

$$\sigma(\mathrm{E})=(\mathrm{l}+1)\sigma_0^{\mathrm{l}+1}(\mathrm{E})\,\chi^{\mathrm{l}+1}(\mathrm{E})+\mathrm{l}\sigma_0^{\mathrm{l}-1}(\mathrm{E})\,\chi^{\mathrm{l}-1}(\mathrm{E})$$

$$\chi^{l}(E)=\frac{1}{(2l+1)\sin^2\delta_l^0}\sum_m \mathrm{Im}\,\tau_{lmlm}^{00}$$

$$\sigma_0^{l}(E)=\frac{8\pi^2}{3}\alpha k\,(E+I_0)\sin^2\delta_l^0\left[\int_0^\infty r^3 R_l(r)\phi_{l_0}(r)\,dr\right]^2$$

atomic cross section - almost without structures and independed from the energy

Final angular momentum according dipole selection rule

$$\mathrm{l}=\mathrm{l}_0\pm 1$$

The scattering path operator can be calculated exactly or by series when the spectral radius ρ less than one

$$(\mathrm{I} - \mathrm{T_a G})^{-1} = \sum_{n=0} (\mathrm{T_a G})^{n}$$

$$\tau = T_a + T_a G T_a G T_a + T_a G T_a G T_a G T_a + ...$$

$$G^{ii}_{LL'} \equiv 0$$

we start from n=2

The size of he spectral radius depends by the energy

MS paths

$$\sigma_n = \sigma_0 \chi_n^l$$

σ_0 – smooth atomic contribution

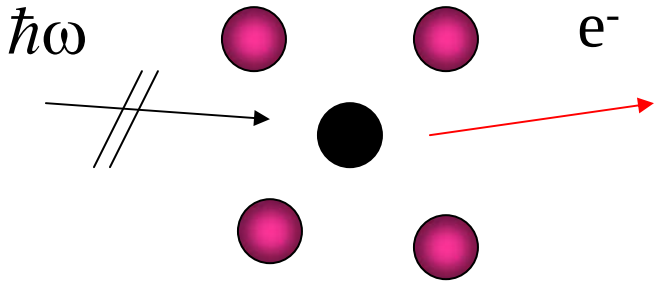

σ_2 – single diffusion – EXAFS region

$$t_l^0 G\, t_l^i G\, t_l^0$$

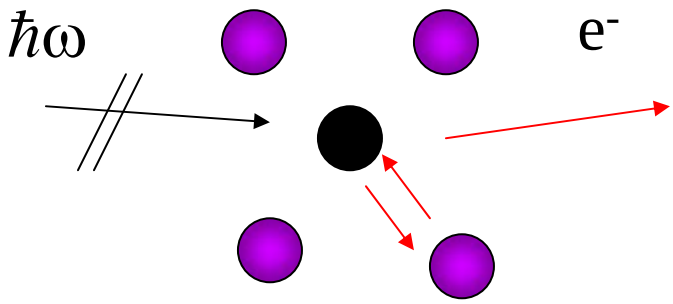

σ_3 – double diffusion – high order correlation functions

$$t_l^0 G\, t_l^i G\, t_{l'}^j G\, t_l^0$$

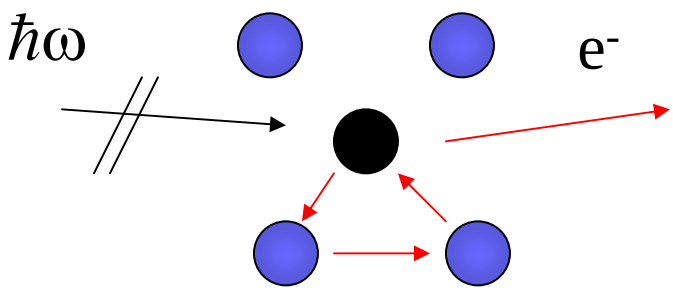

All the structural information are contained in the structural factor

$$\chi^{l}(E) = 1 + \sum_{n=2} \chi_{n}^{l}(E)$$

$$\chi_{n}^{l}(E) = \frac{1}{(2l+1)\sin^{2}\delta_{l}^{0}} \sum_{m} \mathrm{Im}[(T_{a}G)^{n} T_{a}]_{lmlm}^{00}$$

partial contribution of order n coming from all process where the photoelectron is scattered n-1 time by the surrounding atoms before escaping to free space after returning to absorbing atom

The interpretation in term of series is valid only if

$$\rho \leq 1$$

In general

$$\rho \xrightarrow[k \to \infty]{} 0 \qquad (t_l \to 0)$$

$$\rho \xrightarrow[k \to 0]{} \infty \qquad (G \to \infty)$$

High energy $\rightarrow$ σ_0 or $\sigma_0 + \sigma_2$

Low energy $\rightarrow$ $\sigma_0 + \sigma_2 + \sigma_3 + ...$

XAS spectrum – three regions

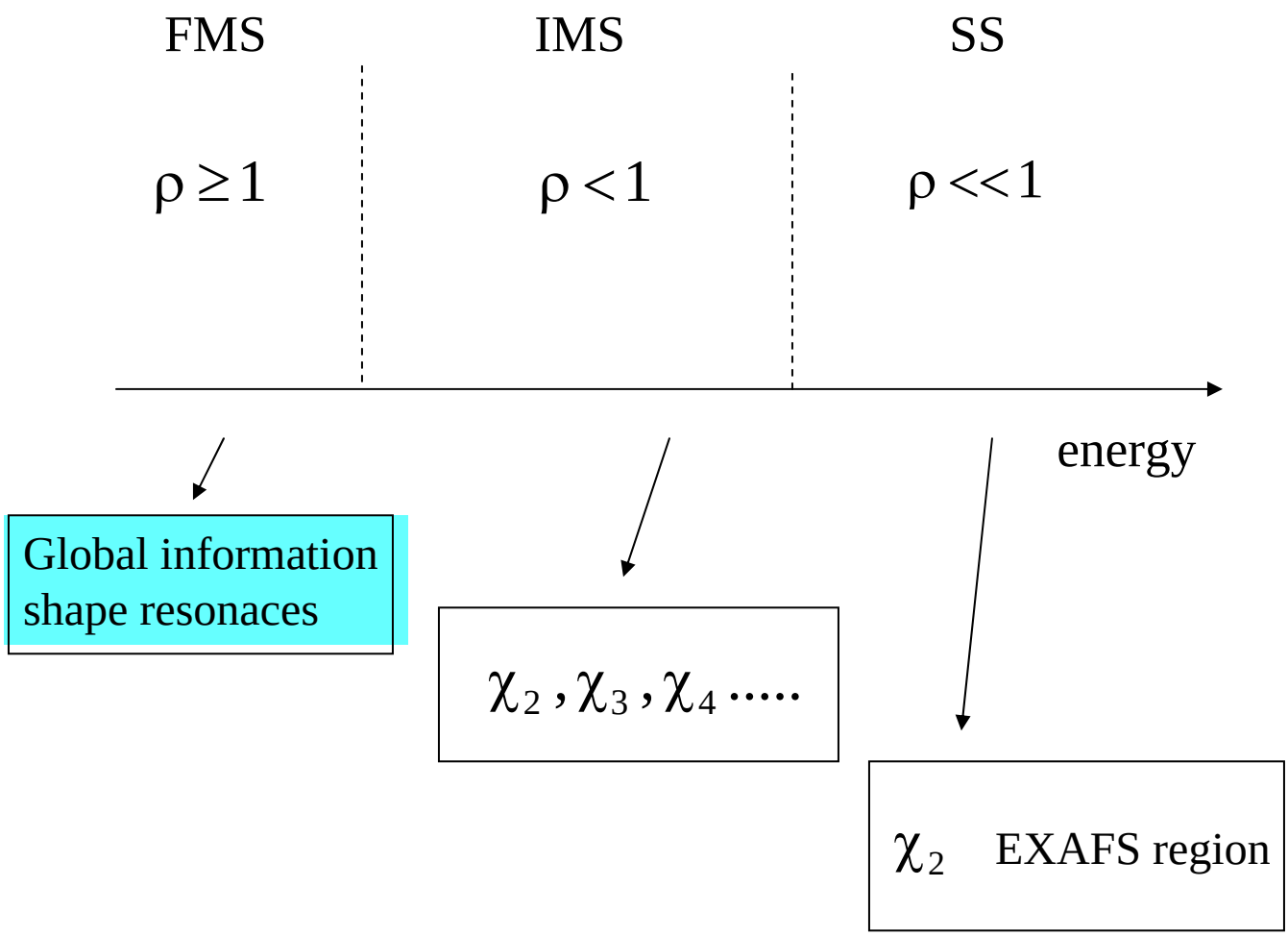

The calculation of the EXAFS signal

$$\chi_2^l = \frac{1}{2l+1} \sum_{j \neq 0} \sum_{m m' l'} \mathrm{Im}\{ e^{2i\delta_l^0} G_{l m l' m'}^{0\,j} t_{l'}^{j} G_{l' m' l m}^{j\,0} \}$$

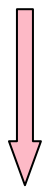

$$\chi_2^l = (-1)^l \sum_{j \neq 0} \sum_{l'} \mathrm{Im}\{ e^{2i\delta_l^0} (i)^{2l'+1} t_{l'}^{j} (2l'+1) H(l, l', kR_{j0}) \}$$

where

$$H(l, l', kR_{j0}) = \sum_{l''} (i)^{l''} (2l''+1) \begin{pmatrix} l & l' & l'' \\ 0 & 0 & 0 \end{pmatrix}^2 (h_{l''}^{+}(kR_{j0}))^2$$

All other signals can be derived in the same way by 3j, 6j, 9j symbols.

Plane wave approximation

$$(i)^l \, h_l^+(kR) \rightarrow \frac{e^{ikR}}{kR}$$

$$\chi_2^l = (-1)^l \sum_{j \neq 0} \mathrm{Im}\{e^{2i\delta_l^0} \, \frac{e^{2ikR_{j0}}}{kR_{j0}} F_j(k)\}$$

$$F_j(k) = \frac{1}{k} \sum_l (i)^{2l+1} (2l+1) e^{i\delta_l^j} \sin \delta_l^j$$

The phase does not depend by the distance

Mn K-edge

M. Benfatto et al. PRB **34** (1986)

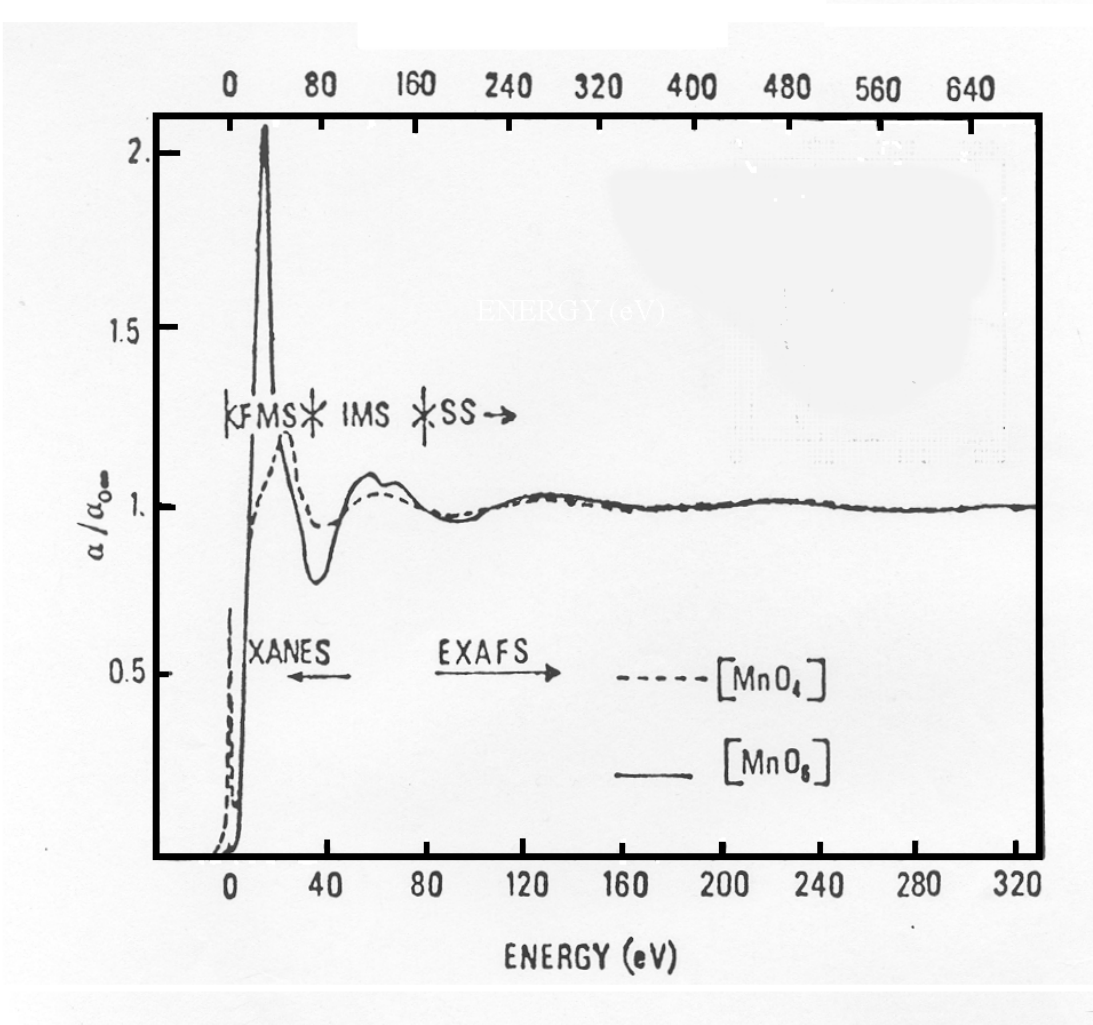

The energy scale are in the ratio 0.47 to account for the different distance between Mn and O in MnO_6 and MnO_4

The amplitude has been corrected for the different number of neighbourings

The two spectra are the same beyond 150 eV → MS contributions

There are cases where $\rho \approx 1$ around 100-150 eV

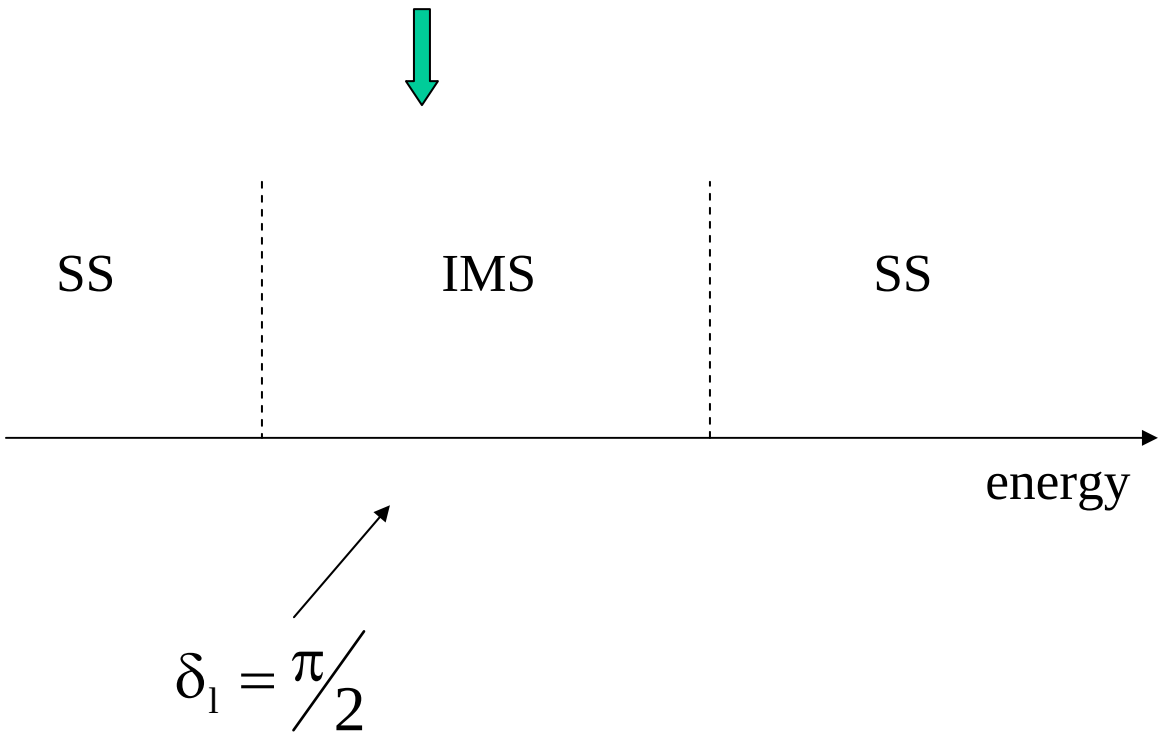

the k-edge of transition metals

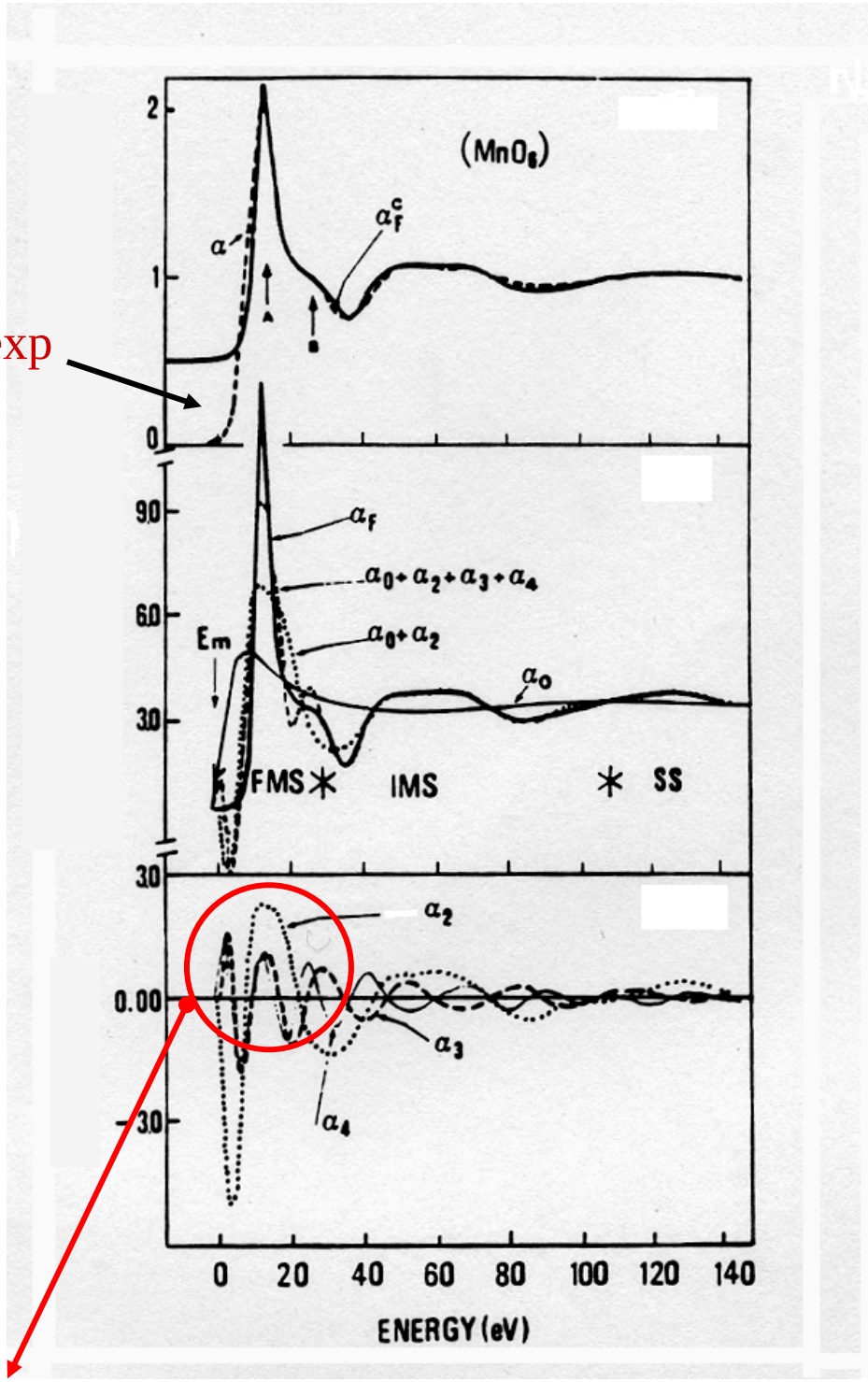

All the MS contributions are at the same energy

Shape resonance

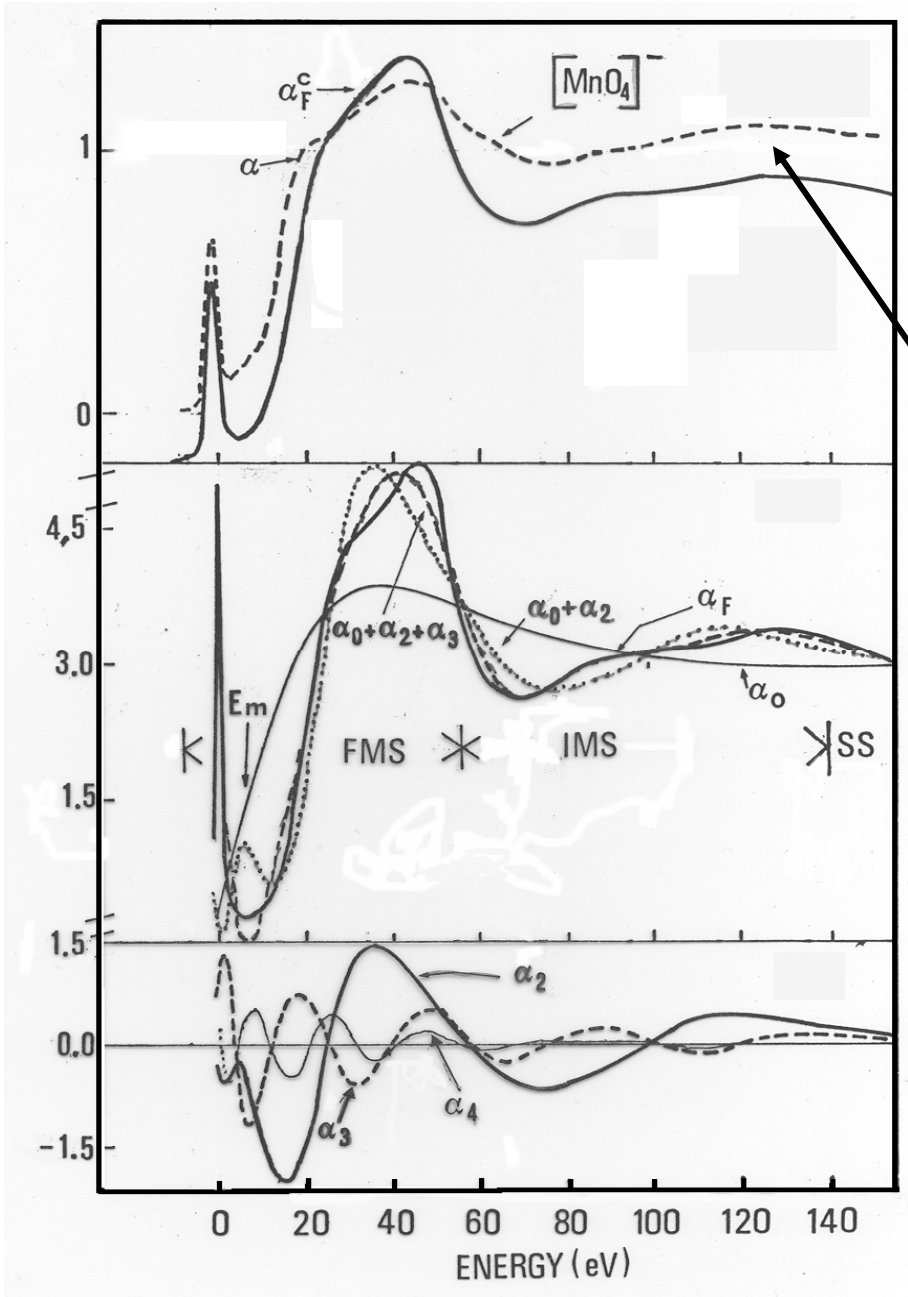

exp

Tetrahedral coordination

Relevant MS contributions up to 150 eV

FMS region

- MS series does not converge $\rho \geq 1$

Many or infinite number of paths contribute to the shape of the spectrum - usually near the edge region (20-40 eV from the edge) for low Z scattering atoms

The scattering path operator must be calculated exactly

Shape resonance global information

point group symmetry - relations like $k_r R$=const.

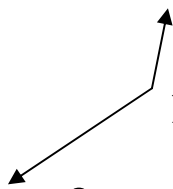

Resonance condition

$$\tau = \left[M - i\Delta\right]^{-1} \qquad \mathrm{Det}M(E_r) = 0$$

Mn K-edge in MnO_4

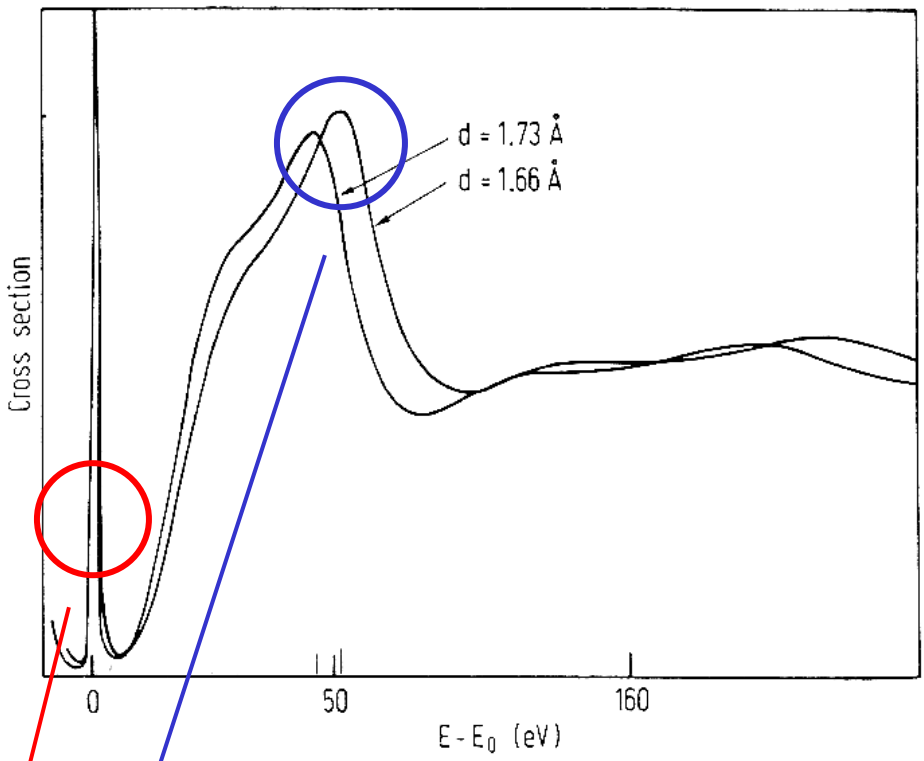

$$\left|E_b - E_r\right| R^2 = \text{const}$$

139.8 for d=1.73

142.3 for d=1.66

IMS and SS regions $\rho < 1$

Typically from 30 eV above the absorption edge

Information on bond lengths and angles

The photoelectron is sensitive to the relative position of two, three or more atoms at the time via the MS paths

Experimental analysis in term of partial contribution $\chi_n^l(E)$

Each term can be written using the (3n-3)-j symbols

Very complicated expressions

but

the functional form

$$\chi_n^l(E) = \sum_{p_n} A_n^l(k, R_{ij}^{p_n}) \sin[kR_{p_n}^{tot} + \varphi_n^l(k, R_{ij}^{p_n})]$$

one can always fit an experimental spectrum with a series of EXAFS like functions.

It is used for making configurational average

Debye-Waller factors

Structural disorder

MnO_4

χ_3 signal

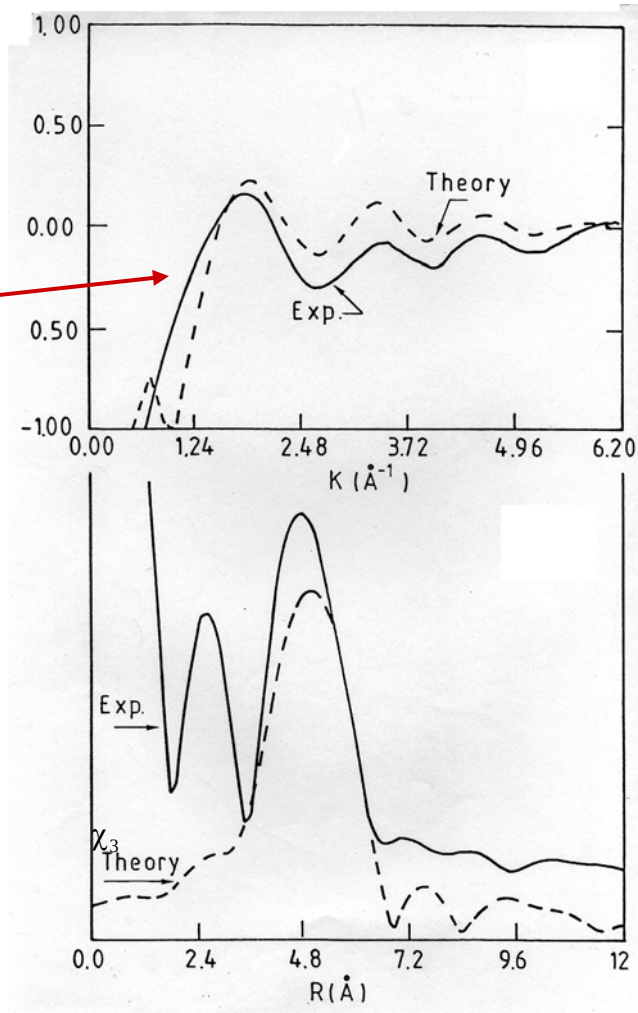

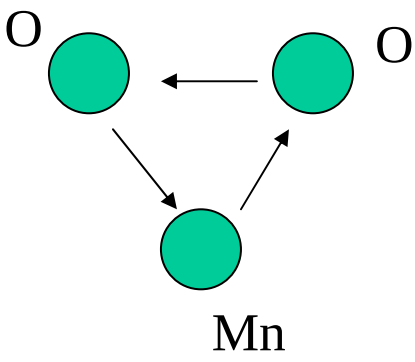

R_{tot} (exp) = 5.65

R_{tot} (theo) = 5.85

Real value = 5.87

$GeCl_4$

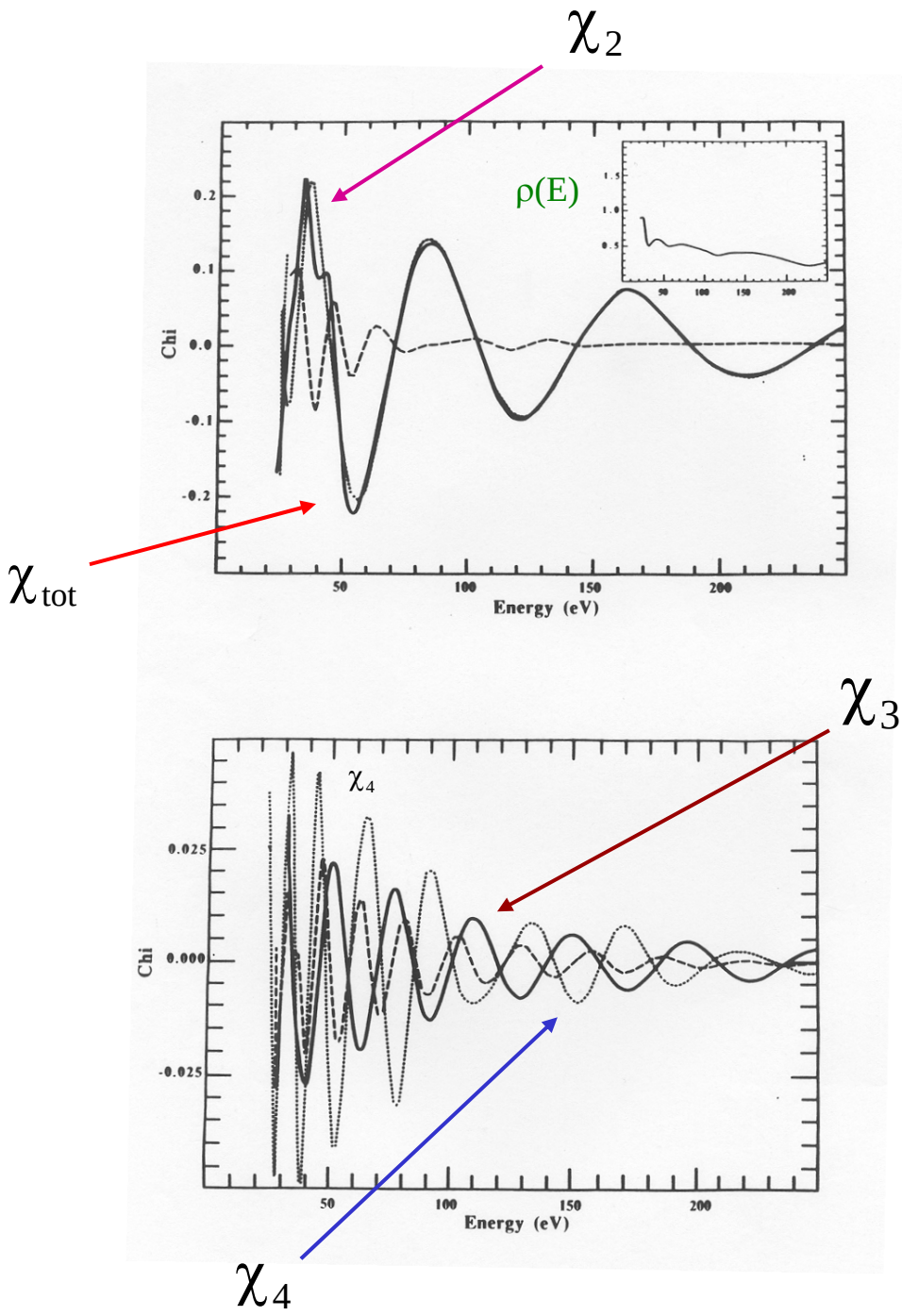

Each individual MS signal has big amplitude

Their sum is affected by massive cancellation

some conclusions

- Core levels are spatially localized
- Every atom has a well defined core levels

site selectivity

The photoelectron probes the system

Strong interaction with the matter

Infomation beyond the pair correlation functions

We need to account for other physical processes

- inelastic excitations suffered by the photoelectron
- electronic excitations due to the creation on core-hole
- finite core hole width
- …….

They drain away amplitude from the elastic channel and must be included in any realistic calculation

finite lifetime of the photoelectron in the final state

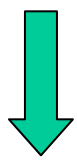

many-body treatment of the photoabsorption process

Band structure calculations

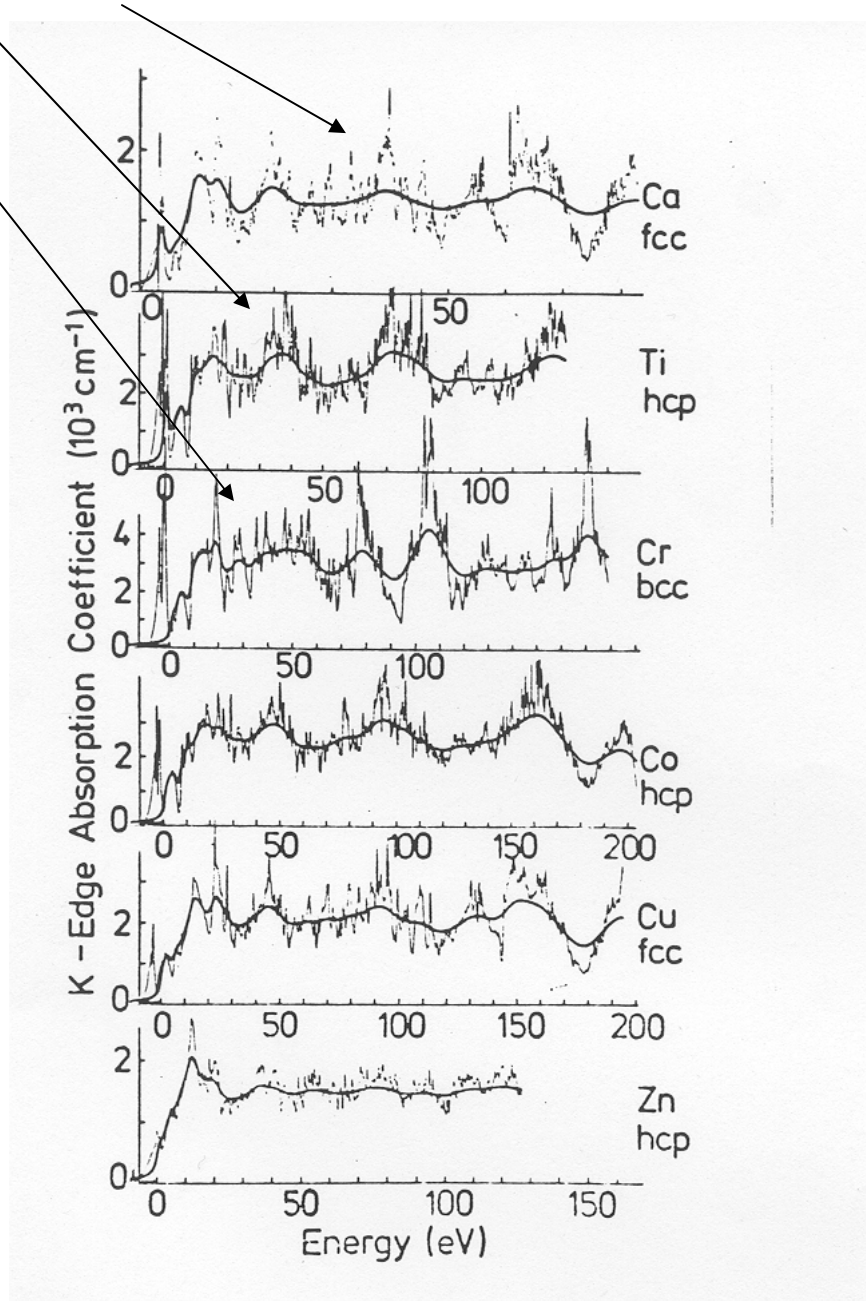

We need to put inelastic looses in the calculations

$$\sigma(\omega) = 4\pi^2 \alpha\, \omega \sum_f \left| \left\langle \Psi_f^N \left| \vec{\varepsilon} \cdot \vec{r} \right| \Psi_G^N \right\rangle \right|^2 \delta(\omega - E_f + E_c)$$

Many body final and ground state w.f.

$$\Psi_G^N(\vec{r}, \vec{r}_1 \ldots \vec{r}_{N-1}) = \sqrt{N!}\, A\, \phi_{L_0}^c(\vec{r}) \Psi_G^{N-1}(\vec{r}_1 \ldots \vec{r}_{N-1})$$

antisymmetrization operator

core level

$$\Psi_G^{N-1}(\vec{r}_1 \ldots \vec{r}_{N-1}) = \sum_n C_n \phi_n^{N-1}(\vec{r}_1 \ldots \vec{r}_{N-1})$$

Slater determinants

for the final state

$$\Psi_f^N(\vec{r},\vec{r}_1...\vec{r}_{N-1}) = \sqrt{N!}\,A\sum_\alpha \phi_\alpha^f(\vec{r})\Psi_\alpha^{N-1}(\vec{r}_1...\vec{r}_{N-1})$$

excited photoelectron

final state channels w.f. relaxed around the core hole

$$H_{N-1}\Psi_\alpha^{N-1} = E_\alpha^{N-1}\Psi_\alpha^{N-1}$$

$$(\nabla^2 + k_\alpha^2)\phi_\alpha^f(\vec{r}) = \sum_\beta \int V_{\alpha\beta}(\vec{r},\vec{r}')\,\phi_\beta^f(\vec{r}')\,d\vec{r}'$$

where

$$k_\alpha^2 = \omega - I_c - \Delta E_\alpha$$

Interchannels potential depending also to non-local exchange term

ionization potential

excitation energy left behind in the (N-1) particle system

It is convenient to introduce the Green functions writing the total photoabsorption cross section

$$\sigma(\omega) \propto \sum_{m_0,\sigma_0} \int d^3r d^3r' \phi^c_{L_0}(\vec{r})\, \vec{\varepsilon}\cdot\vec{r}\; \mathrm{Im}\left\{ \sum_{\alpha,\alpha'} S^*_\alpha S_{\alpha'} G_{\alpha,\alpha'}(\vec{r},\vec{r}';\omega - I_c) \right\} \vec{\varepsilon}\cdot\vec{r}'\, \phi^c_{L_0}(\vec{r}')$$

$$S_\alpha = \left\langle \Psi^{N-1}_\alpha \middle| \Psi^{N-1}_G \right\rangle$$

$$G_{\alpha,\alpha'}(\vec{r},\vec{r}';E) = \sum_f \frac{\phi^f_\alpha(\vec{r})\phi^f_{\alpha'}(\vec{r}')}{E - \Delta E_f - i\eta}$$

$$\Delta E_f = E_f - E_G$$

$$E_f = E_G + \omega$$

The Green's-functions matrix satisfies a set of coupled equations that contains the complete description of all the possible outcomes of a photoemission process

Two possibilities

the complete relaxed channel dominates $\Delta E_\alpha = 0$

$$\sigma(\omega) \propto \mathrm{Im}\left|S_0(\omega)\right|^2 G_{00}(\omega - I_c)$$

Different channels

$$\sigma(\omega) \propto \mathrm{Im} \sum_{\alpha,\alpha'} M_L^{\alpha}\ \tau_{0L,0L}^{\alpha,\alpha'}\ M_L^{\alpha'}$$

$$\tau = S^{-1}$$

$$S = \begin{matrix} [\tau_o^{-1}]^{\alpha_0} & [K^{-1}]^{\alpha_0\alpha_1} & .. \\ [K^{-1}]^{\alpha_1\alpha_0} & [\tau_o^{-1}]^{\alpha_1} & .. \\ .. & .. & .. \end{matrix}$$

τ_o is the usual scattering path operator for the channel α with the k_α wave-vector

If only one electronic configuration dominates, typically the complete relaxed channel $\Delta E_\alpha = 0$

We can eliminate from the set all channels which give rise to similar interchannels potential

Plasmon type – delocalized in the system

$$\sigma(\omega) \propto \mathrm{Im}\left|S_0(\omega)\right|^2 G_{00}(\omega - I_c)$$

it satisfies a Dyson equation with optical potential

$$\left[\nabla^2 + E - V_c(\vec{r}) - \Sigma_{exc}(\vec{r};E)\right] G^+_{00}(\vec{r},\vec{r}';E) = \delta(\vec{r}-\vec{r}')$$

$$\Sigma_{exc}(\vec{r};E) = V(\vec{r};E) + i\Gamma(\vec{r};E)$$

from many body to on effective one particle problem

Some considerations

- in metal one obtains very good agreement with the experimental data using a one-particle approach with an X-α potential and convoluting the calculated spectrum with a Lorentzian broadening function having an energy-dependent width.

- double-electron excitations are normally very weak, typically 10^{-2} – 10^{-3} times the main relaxed channel

we choose the Hedin-Lundqvist (HL) potential extending its validity in to the atomic core region

it has an imaginary part that is able to reproduce the observed mean-free path in metal. This part starts at the plasmon energy

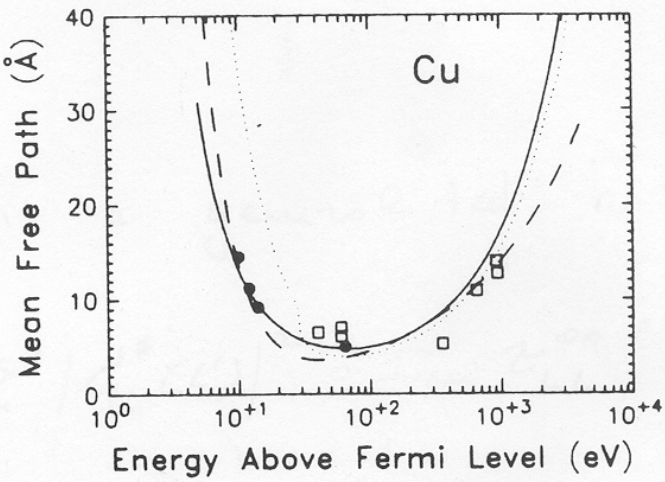

FIG. 1. Inelastic electron mean free path versus energy above the Fermi energy for Cu. Solid curve is present theory. Dotted curve is theory of Tung *et al.* (Ref. 1). Dashed curve is from Seah and Dench (Ref. 8). Experimental data: solid circles, Refs. 10 and 11; open squares, Ref. 14.

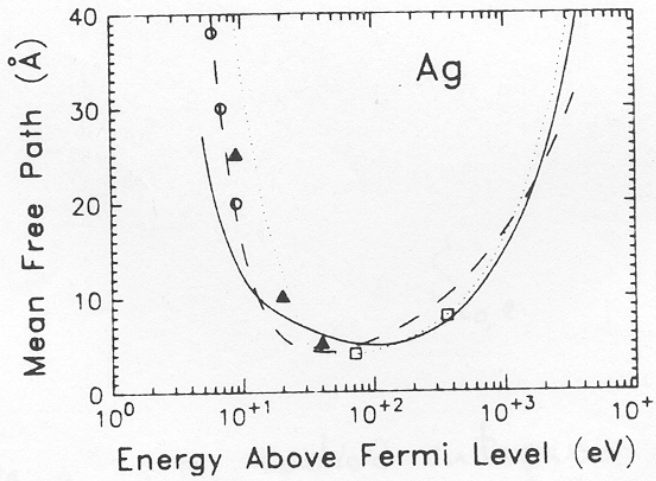

FIG. 2. Same as Fig. 1 but for Ag. Experimental data: open circles, Ref. 15; solid triangles, Ref. 16; open squares, Ref. 17.

Inelastic electron mean free path

For a muffin-tin type of potential

$$G^{+}_{00}(\vec{r},\vec{r}';E) = -k\sum_{L,L'} R^{0}_{L}(\vec{r})\,\tau^{00}_{LL'}\,R^{0}_{L'}(\vec{r}') + \sum_{L} R^{0}_{L}(\vec{r})S^{0}_{L}(\vec{r}')$$

usual scattering path operator

total structural signal in a final angular momentum channel l

$$\chi_l(E) = \frac{\sigma_l(E)}{[\sigma_a(E)]_l} - 1$$

MS signals of order n

$$\chi^{n}_l(E) = \frac{\sigma^{n}_l(E)}{[\sigma_a(E)]_l}$$

The use of complex potential automatically introduces a damping in the the elastic signal

$$G_{LL'}^{ij} \approx \frac{e^{ikR_{ij}}}{kR_{ij}}$$

If $k = k_r + i\,k_i$ we have a decreasing exponential

$$\lambda_{tot} = \frac{1}{k}\frac{E}{\Gamma_{tot}(E)}$$

The presence of several possible electronic excitations beyond the elastic one “creates” the concept of the electronic inelastic mean free path

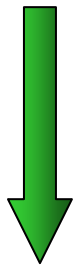

we see only few shells around the absorber typically 5-10 at the edge

To account for that we have introduced an optical potential with a complex part – Within some conditions this is completely equivalent to a convolution of the real calculation

S K-edge in ZnS

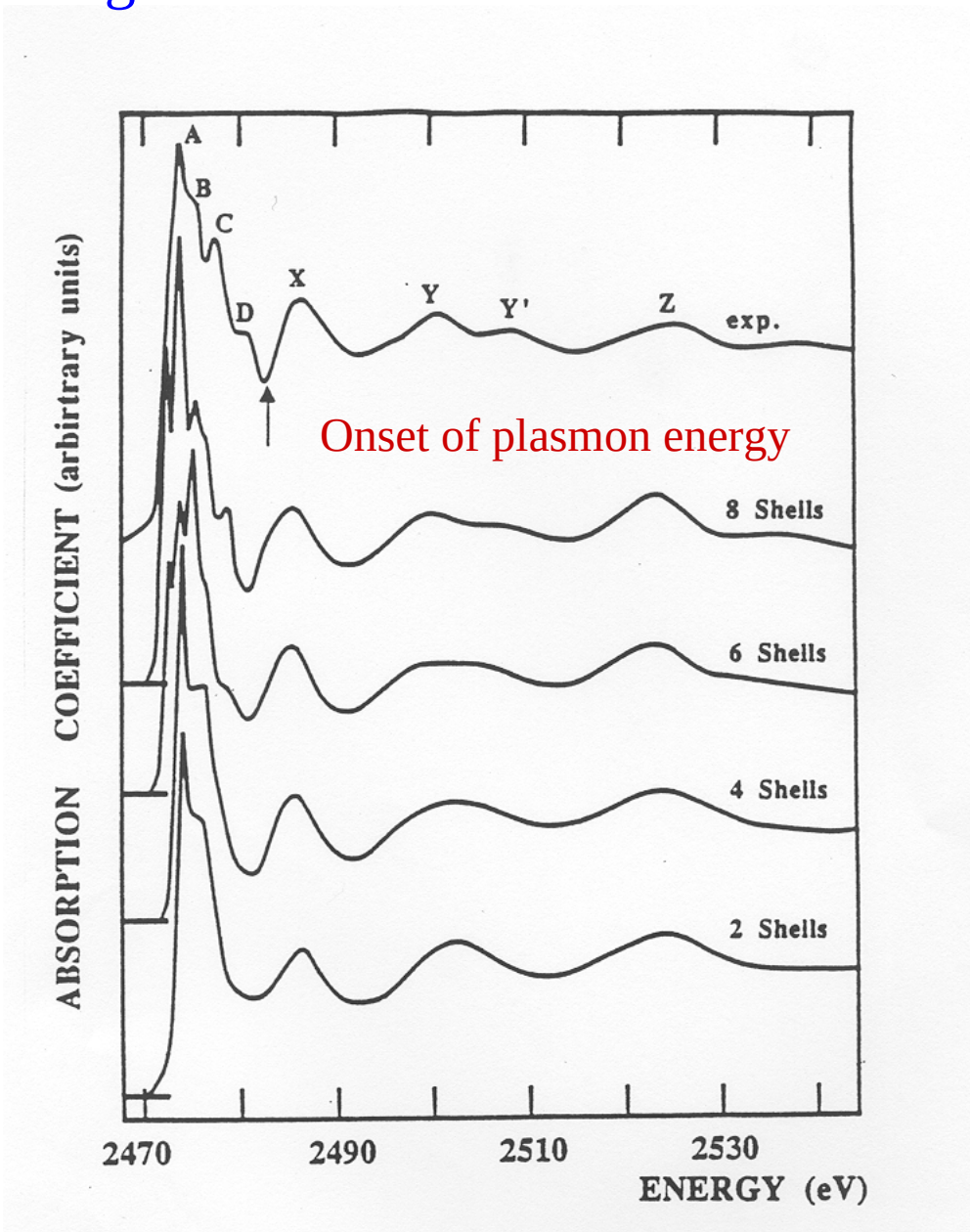

The cross section has been built shell by shell

Si K-edge crystal silicon

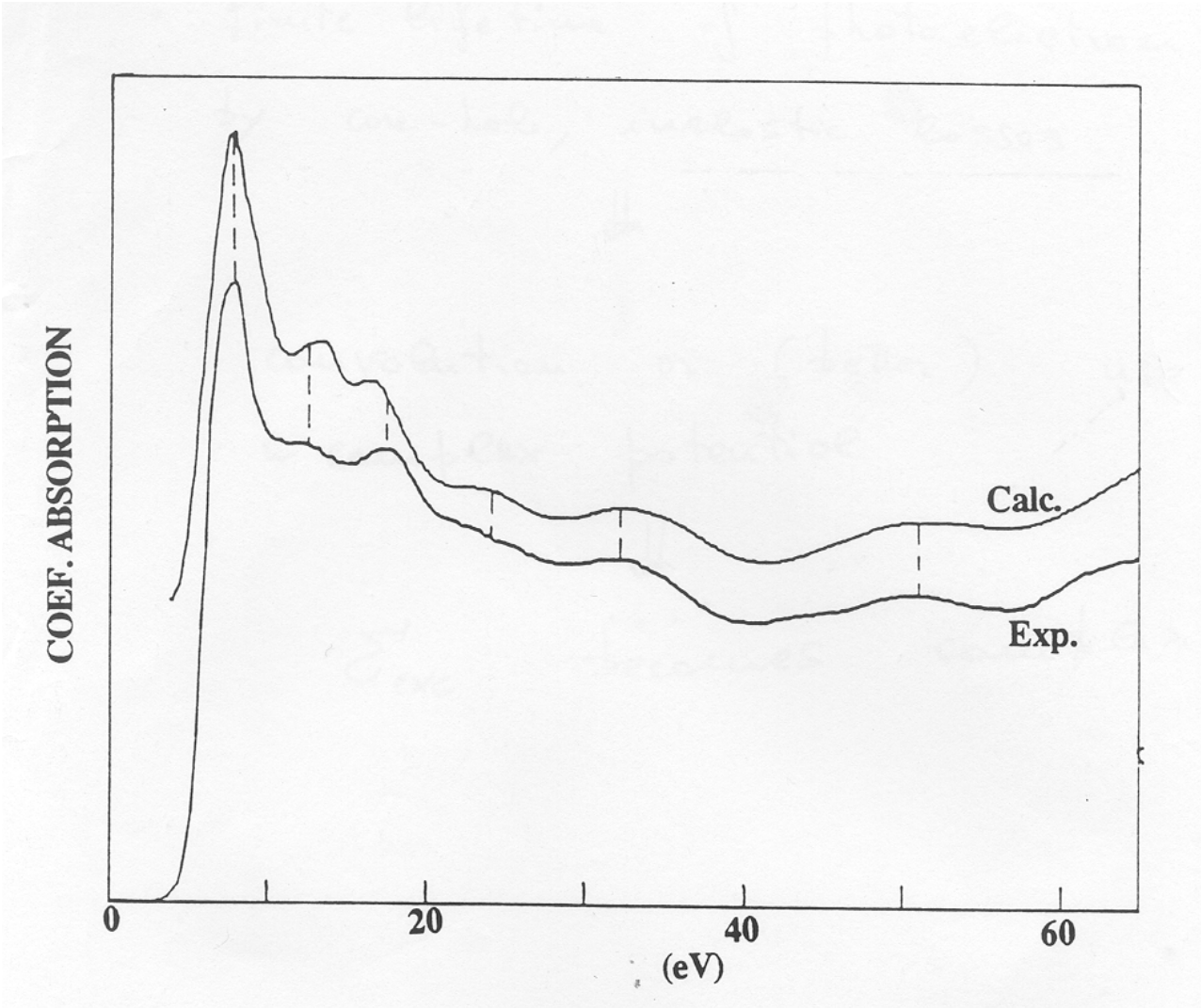

8 shells around the absorber

Na K-edge in NaCl

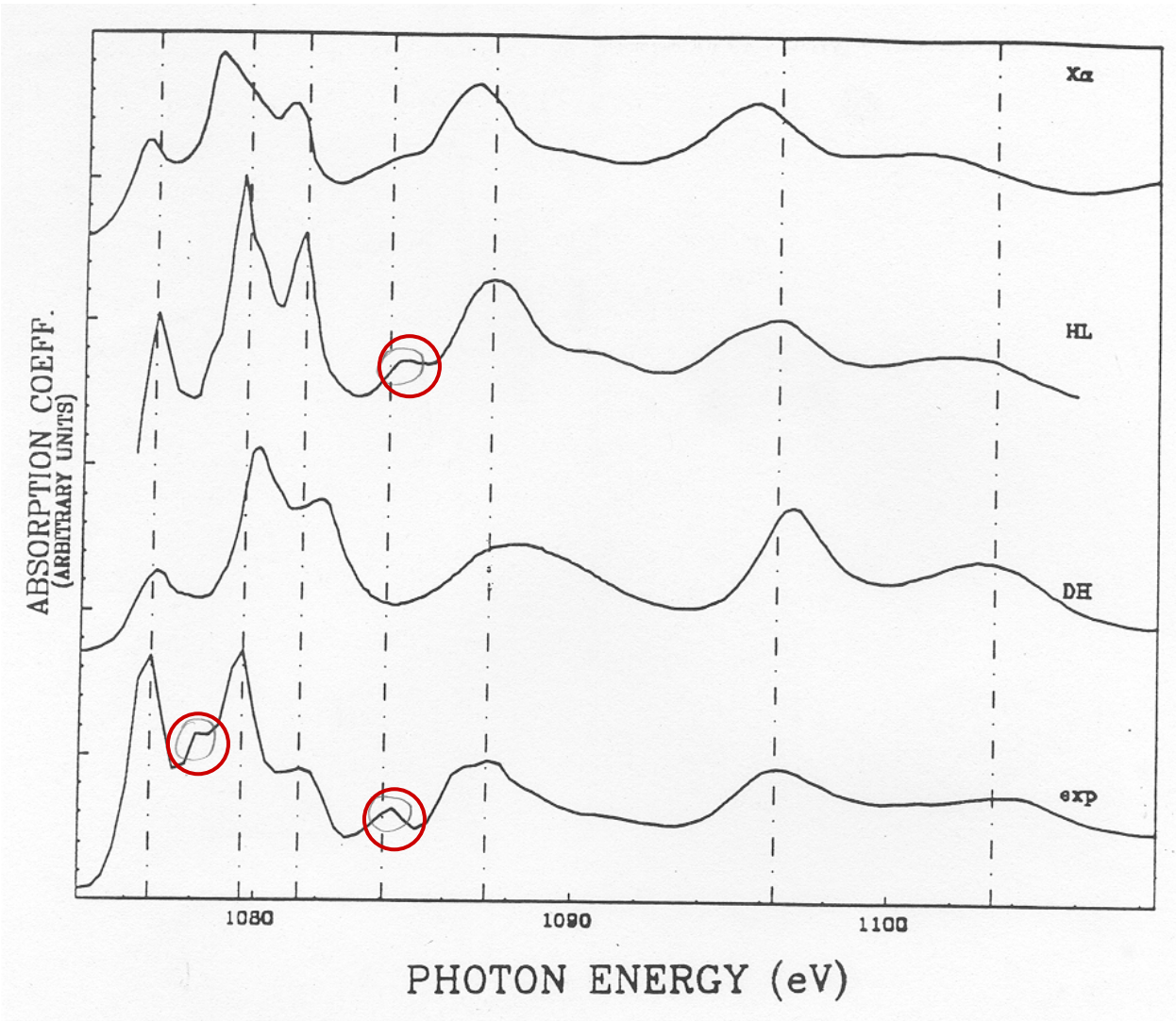

The case of several electronic configurations

Several systems can generate K-edge XANES with "extra" peaks due to the presence of different electronic configurations

Some cuprates – the Cu K-edge – $3d^9 + 3d^{10}\underline{L}$

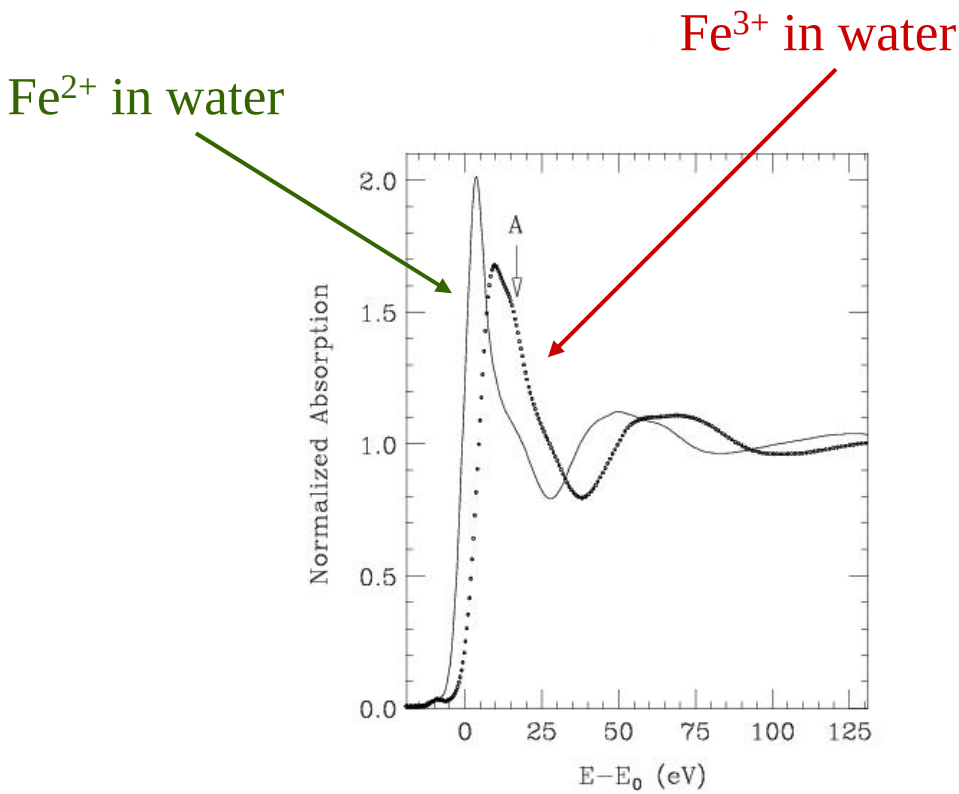

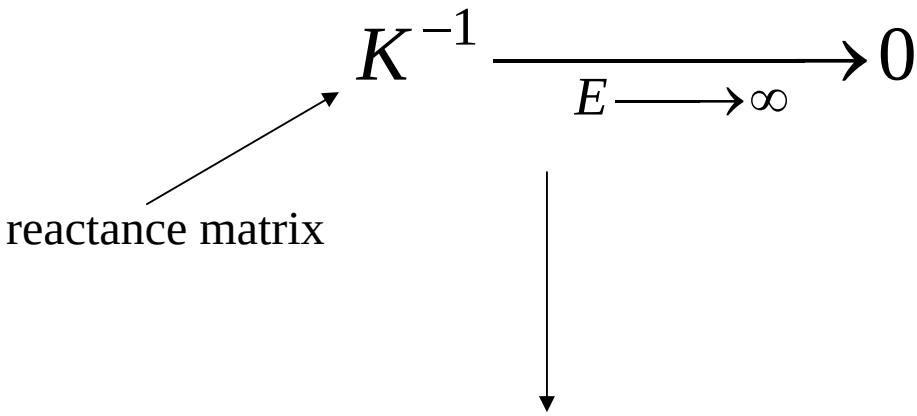

The different channels decouple at high energy

$$\sigma(\omega) = a^2\sigma_0(k_0) + b^2\sigma_1(k_1) + \ldots$$

$$k_0^2 = \hbar\omega - I_c$$

$$k_1^2 = \hbar\omega - I_c - \Delta E_1$$

.....

The total cross section is the sum of independent spectra shifted in energy

experimental data

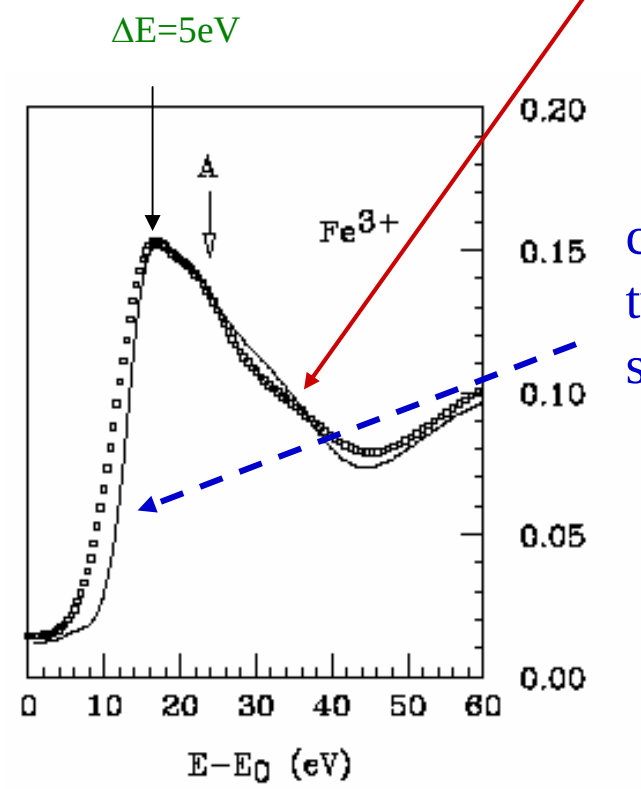

calculation accounting for two configurations in the sudden limit ΔE=5eV

The extra feature A is explained by the presence a second electronic configuration generated by moving one electron from low- to high-t_{2g} level. SCF calculation gives an energy separation ΔE=5 eV

but

Problems for a quantitative structural determination

How to get structural information

Methods essentially based on FT and the concept of phase transferability, normally they are limited to the first shell analysis and systems with negligible MS contribution

These methods use mainly the EXAFS part of the spectrum

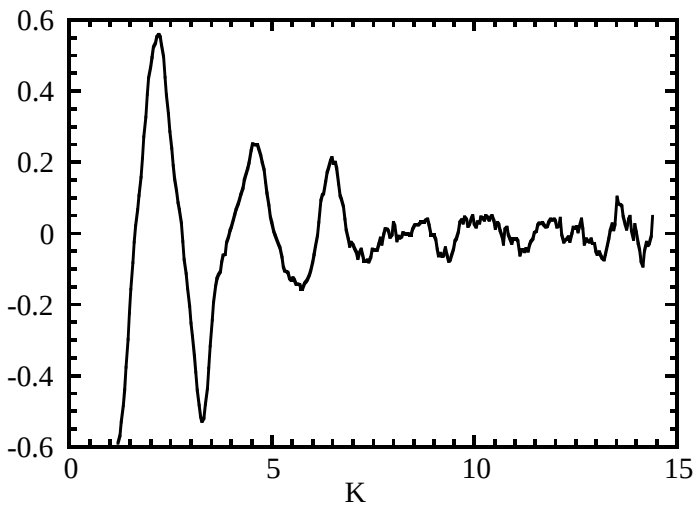

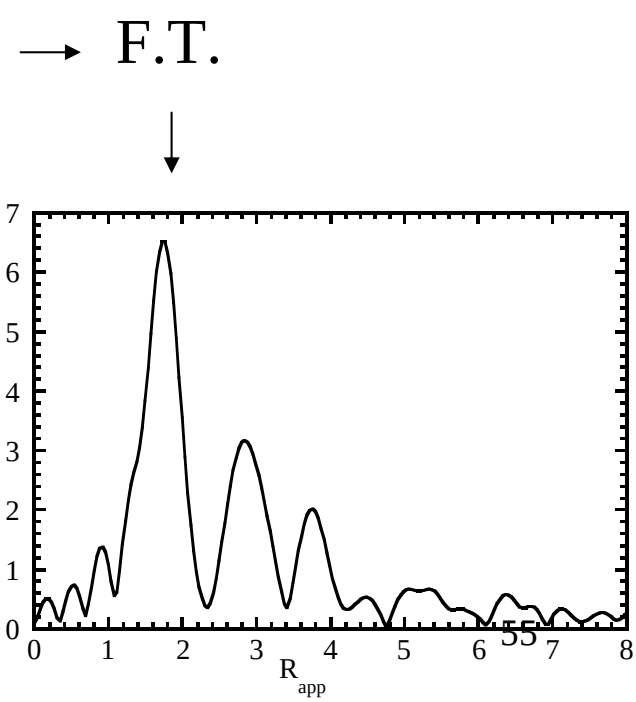

Other methods are based on fit procedure that use the MS approach to generate the theoretical MS series, i.e. χ_n many signals to be compared with exp. data. By moving bond lengths and angles those programs reach the best fit conditions in term of structural used parameters.

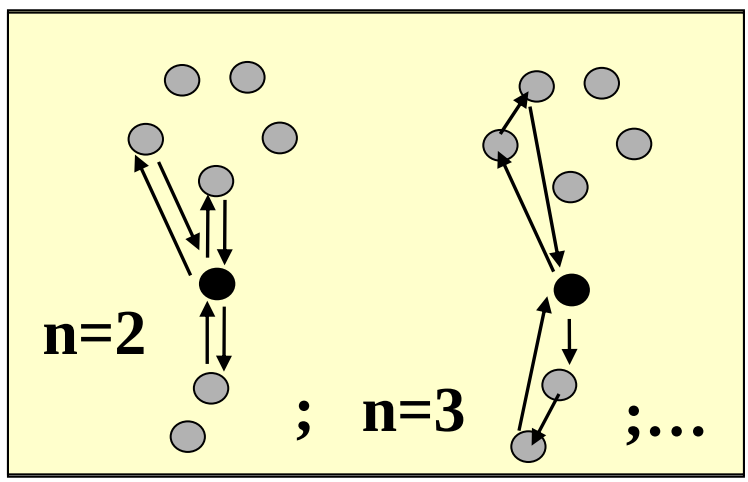

Feff --- EXCURVE

There is the gnXAS program where the χ(K) signal is decomposed into a summation over irreducible n-body signals

$$\chi(0,i,j\cdots,n)=\sum_{i}\gamma^{(2)}(0,i)+\sum_{(i,j)}\gamma^{(3)}(0,i,j)+\sum_{(i,j,k)}\gamma^{(4)}(0,i,j,k)+\cdots$$

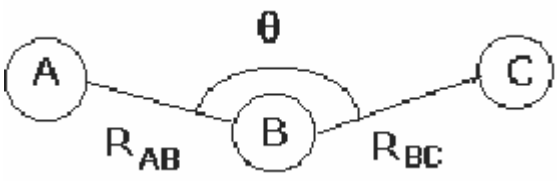

$$\eta^{(3)}=\gamma^{(3)}_{ABC}+\gamma^{(2)}_{AC}$$

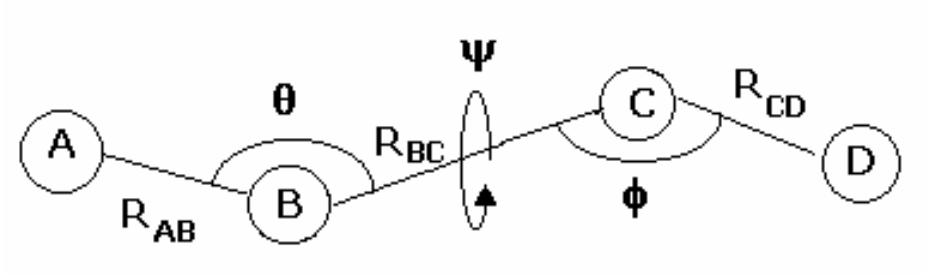

$$\eta^{(4)}=\gamma^{(2)}_{AD}+\gamma^{(3)}_{ACD}+\gamma^{(3)}_{ABD}+\gamma^{(4)}_{ABCD}$$

Multiple scattering signals of the heme plane

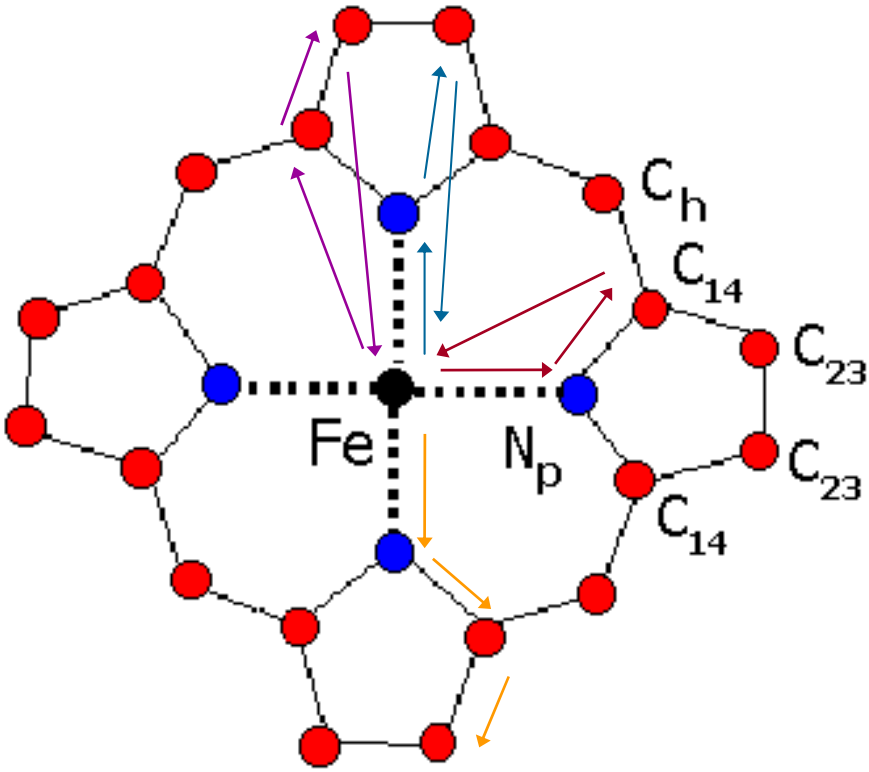

$\gamma^{(3)}$Fe-Np-C_{14}

$\gamma^{(3)}$Fe-N_p-C_{23}

$\gamma^{(3)}$Fe-C_{14}-C_{23}

$\gamma^{(4)}$Fe-Np-C_{14}-C_{23}

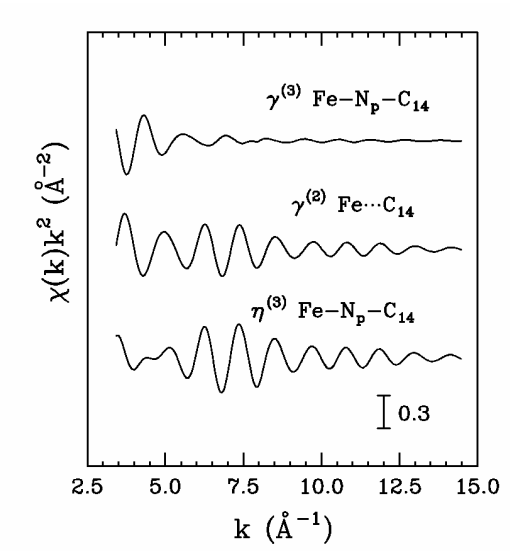

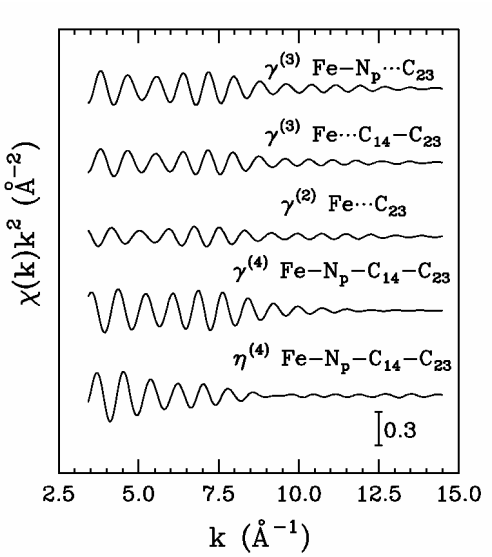

Up to now only a qualitative use of the XANES energy region

The question we want to address:

Is it possible to use XANES (from edge to about 200 eV) as a source of **quantitative** structural information?

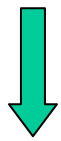

Many XAS spectra “contain” most of the structural information in XANES energy region

We want to weight this part properly in the structural fitting procedure

Biological example

Low temperature photolysis of myoglobin

$$\text{MbCO} \xrightarrow[T < 40K]{h\nu} \text{Mb*CO}$$

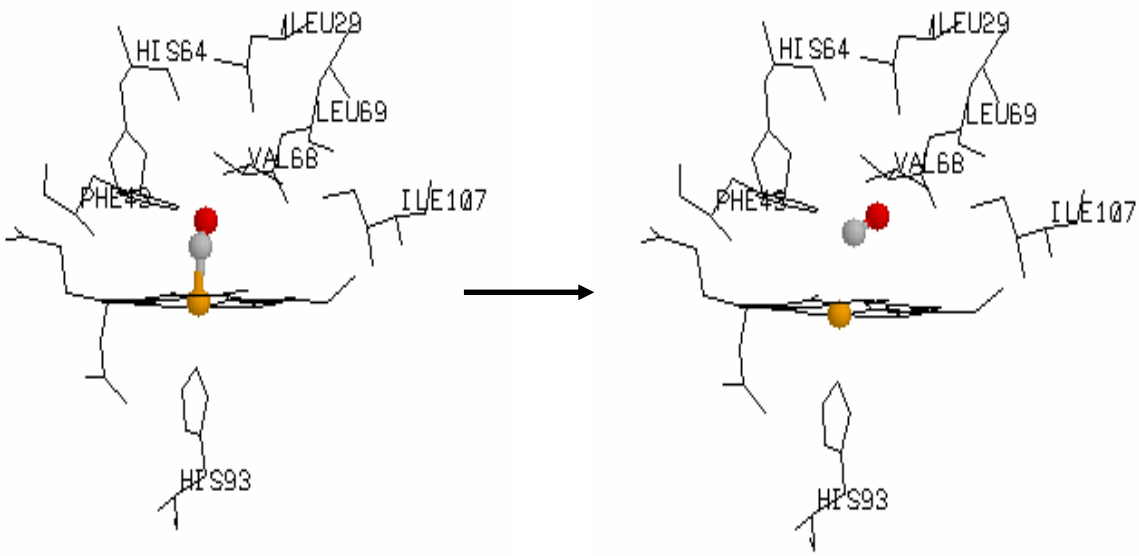

Exp. by S. Della Longa et al. J. Synch. Rad. (1999) **8**, 1138

myoglobin single crystal

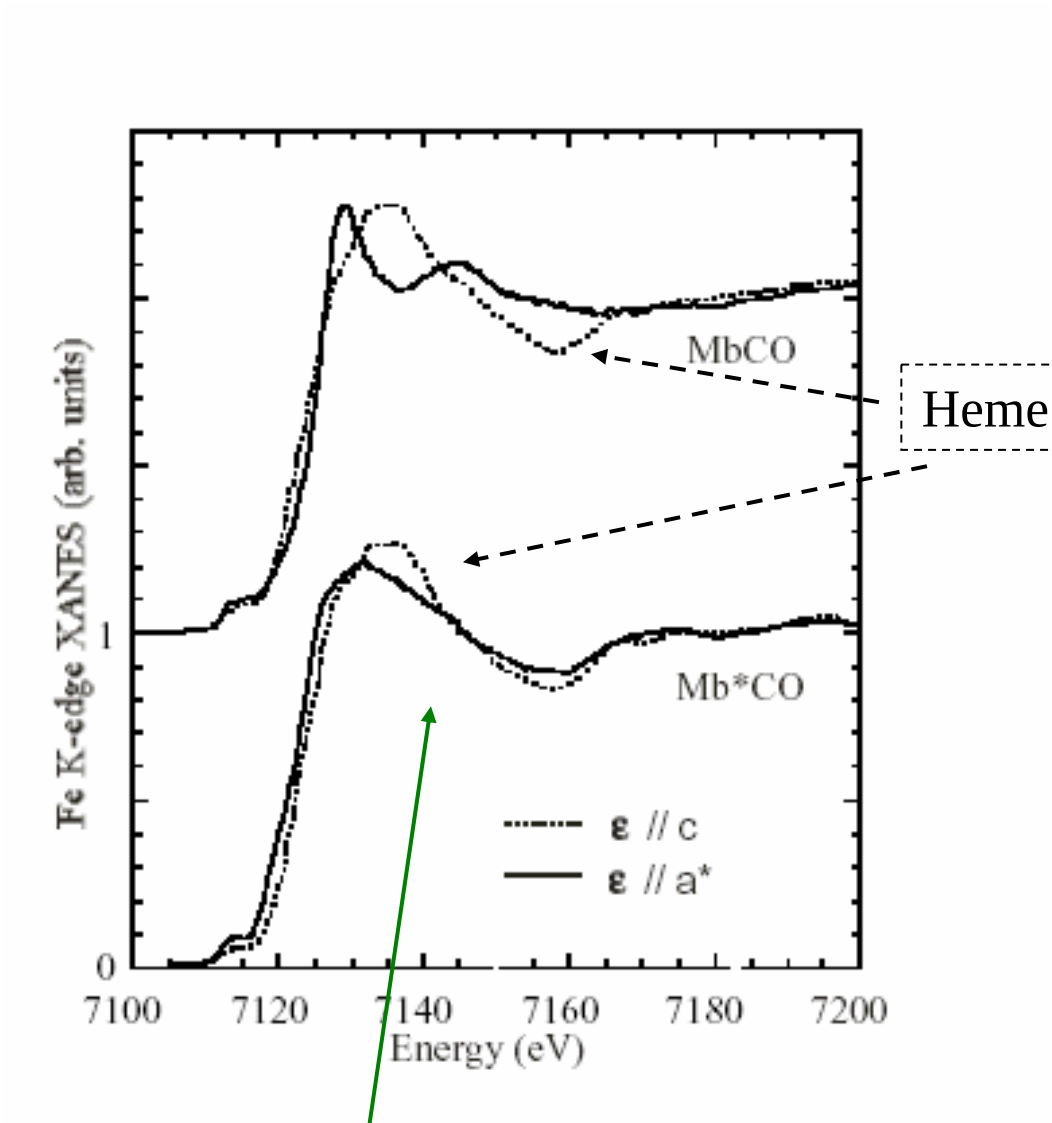

Most of the differences are in the energy range 0 – 80 eV

Two ways to calculate the scattering path operator

Exactly: all MS contributions are included

By series:

$$\sigma(E)=\sigma_0(E)+\sigma_2(E)+\ldots+\sigma_n(E)$$

We have developed a new fitting method that use the exact calculation of the scattering path operator

Most of the actually software packages to make fits use this method

MXAN

i) We work in the energy space
ii) We can start from the edge
iii) We can use polarization dependent spectra

The MXAN method

- Initial geometrical configurations
- Exp. data

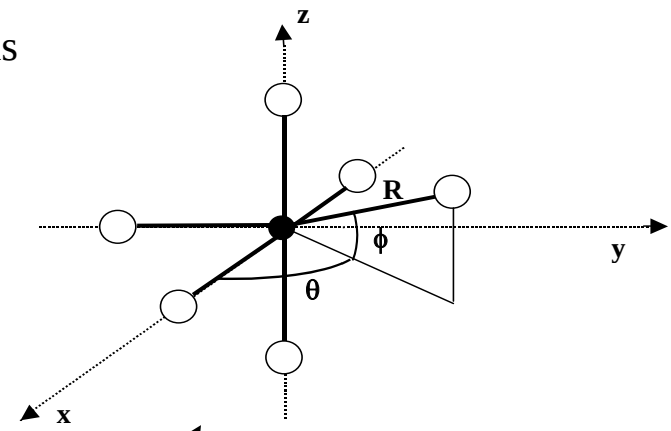

We generate hundred of theor. spectra by moving atomic coordinates

The potential is calculated at each step – Norman criterion

Minimization of error function

$$R_{sq}^{\ 2} = \sum_{i=1}^{N} \{ [y_i^{th.}(..r_n, \theta_n, ..) - y_i^{exp.}]^2 / \varepsilon_i^2 \} w_i / \sum_{i=1}^{N} w_i$$

By comparison with exp. data we can fit relevant structural parameters

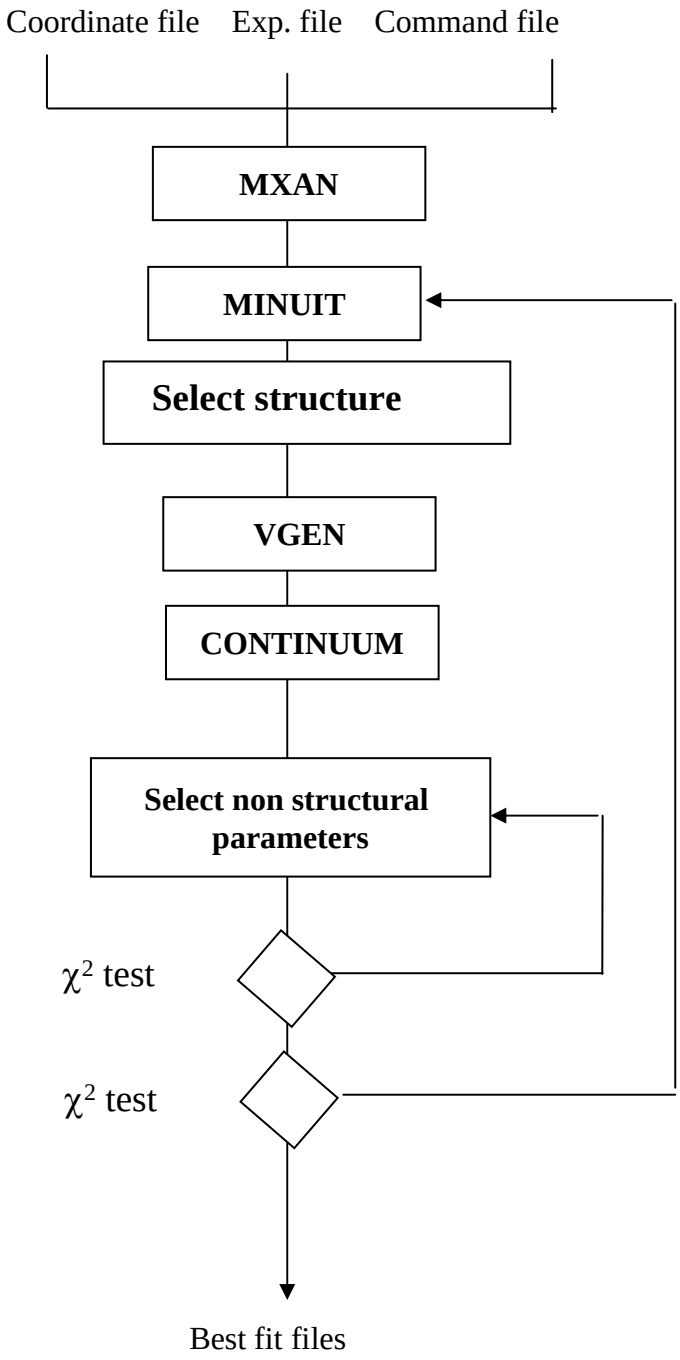
Coordinate file
Exp. file
Command file
MXAN
MINUIT
Select structure
VGEN
CONTINUUM
Select non structural parameters
χ2 test
χ2 test
Best fit files

EXCHANGE and CORRELATION PART

- Complex HL potential + Lorentzian function with a constant Γ_c to account for the core-hole and the experimental resolution

Problems in molecular cluster at low energy, typically in the range 0-30 eV.

Test

Ni^{2+} in water – K-edge of Ni

The calculation at the best fit condition include the H atoms

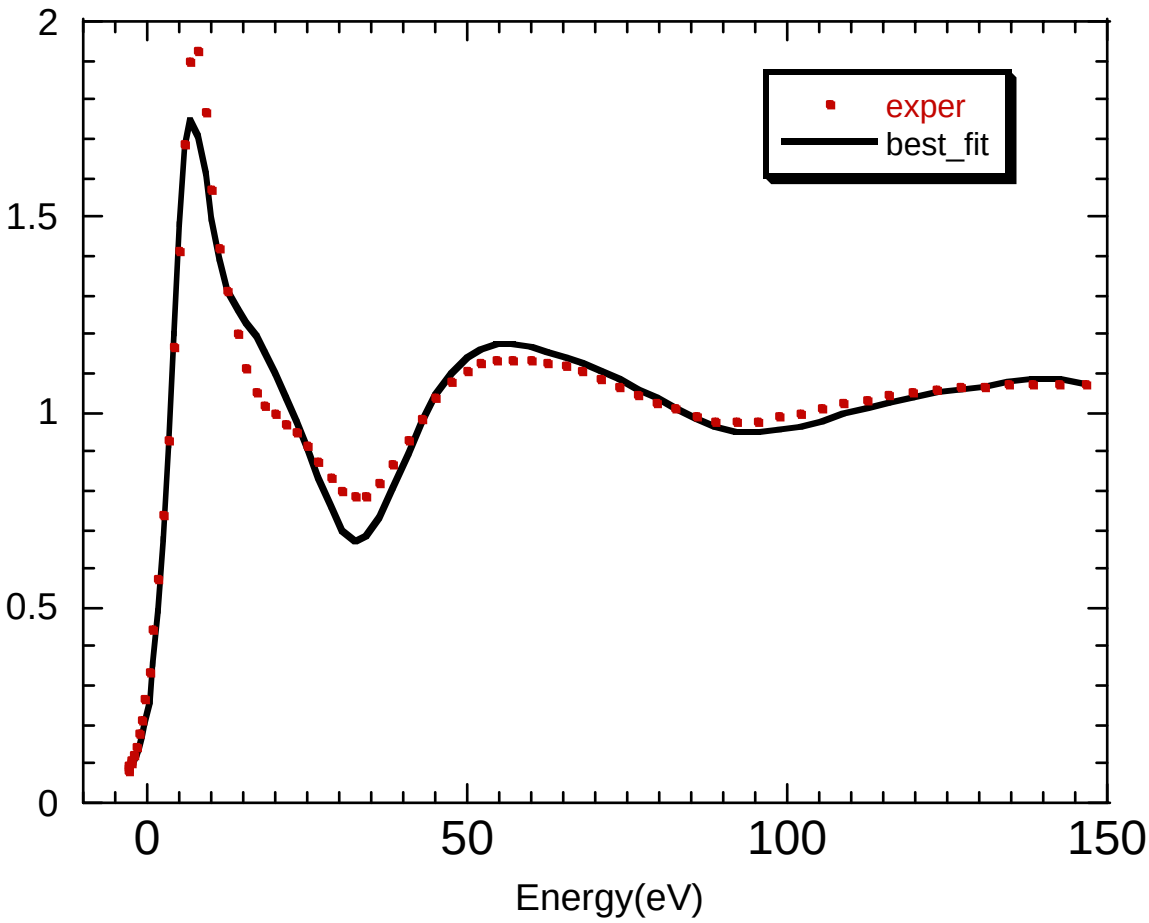

It corresponds to an octahedron with a Ni-O distance of 2.04 Å

The GNXAS and FEFF analysis gives about 2.07 Å

Real HL potential + convolution via a Lorentzian function with $\Gamma_{tot}(E)=\Gamma_c+\Gamma(E)$

$\Gamma(E)$ Behaves like the universal form (Muller et. al., Sol. State Comm. 1982) and starts from energy E_s with a jump A_s. Both E_s, Γ_c and A_s are derived at each step of computation on the basis of Monte Carlo fit.

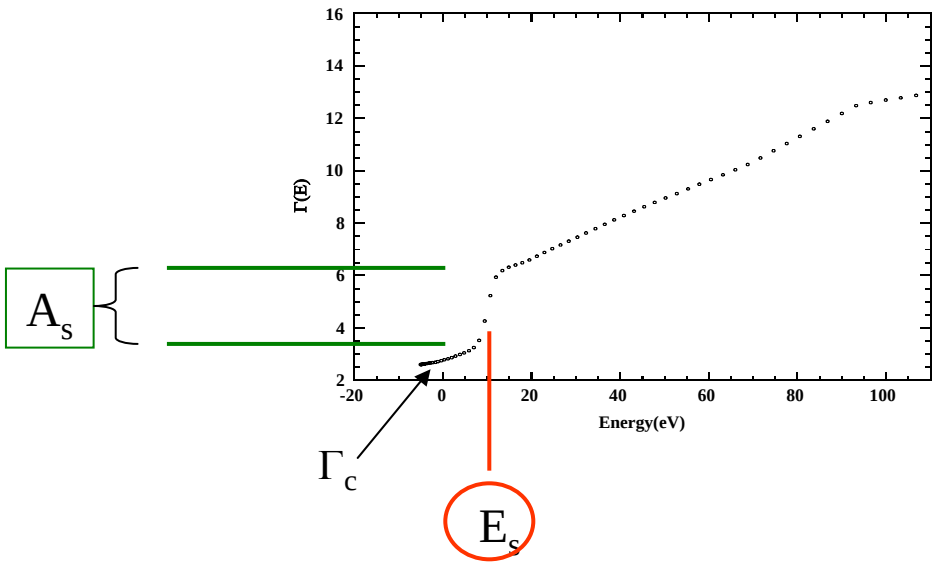

Transition metals in water solution

-Starting condition: distorted orthorhombic symm.
-The fits include Hydrogen atoms

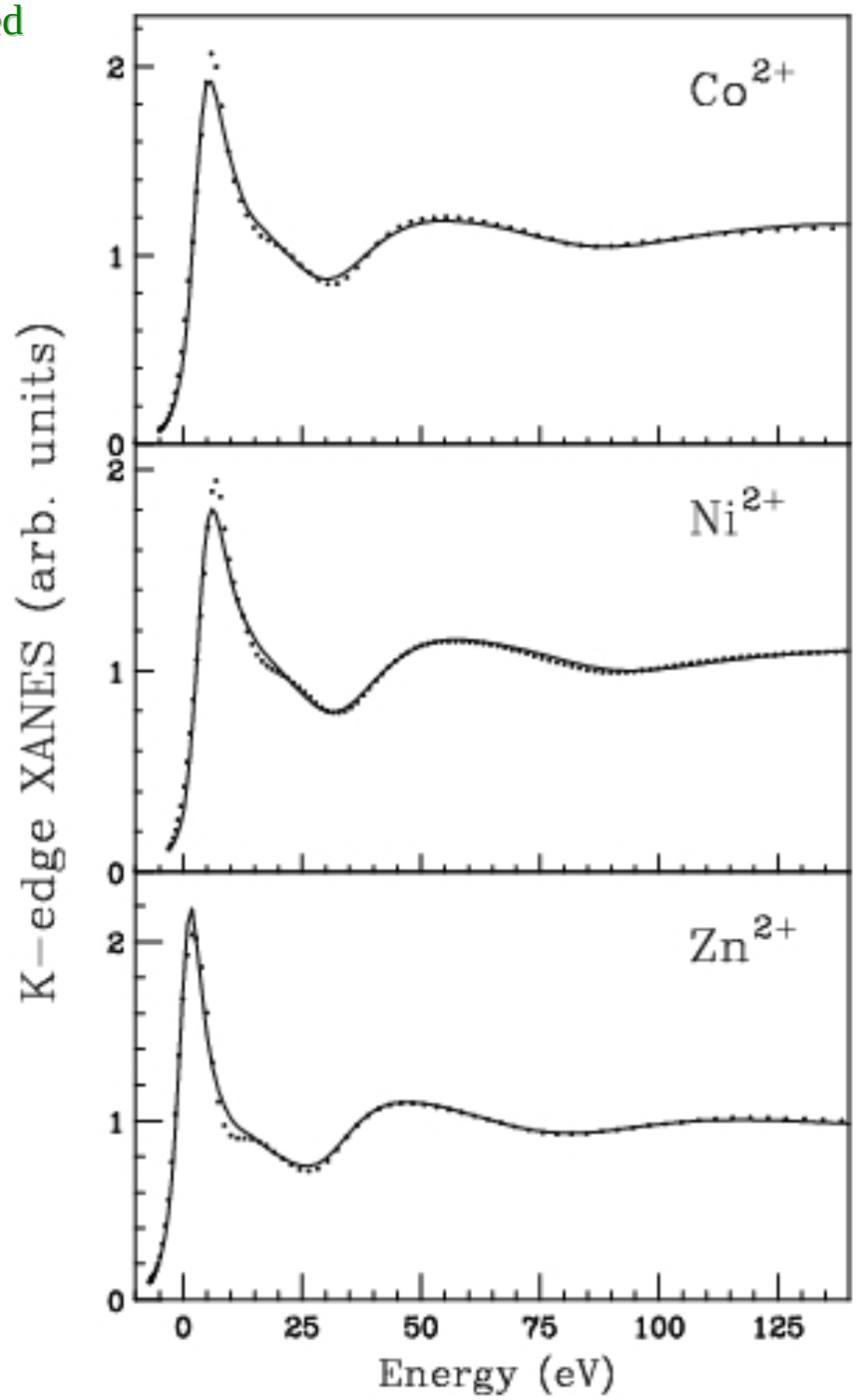

Best fit conditions

Octahedral symmetry

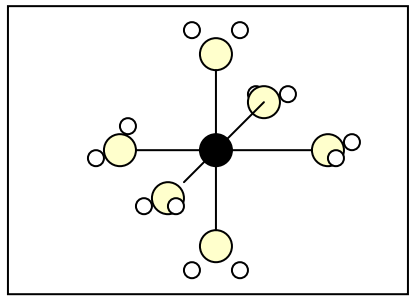

	R(Å)	R(Å)	Γ_c	$\Gamma_{c\text{-}h}$
Co^{2+}	2.06(0.03)	2.092(0.002)	2.07	1.33
Ni^{2+}	2.03(0.03)	2.072(0.002)	1.70	1.44
Zn^{2+}	2.06(0.02)	2.078(0.002)	3.14	1.67

MXAN

GNXAS

Fit with Zn R_{mt}=1.2 Å

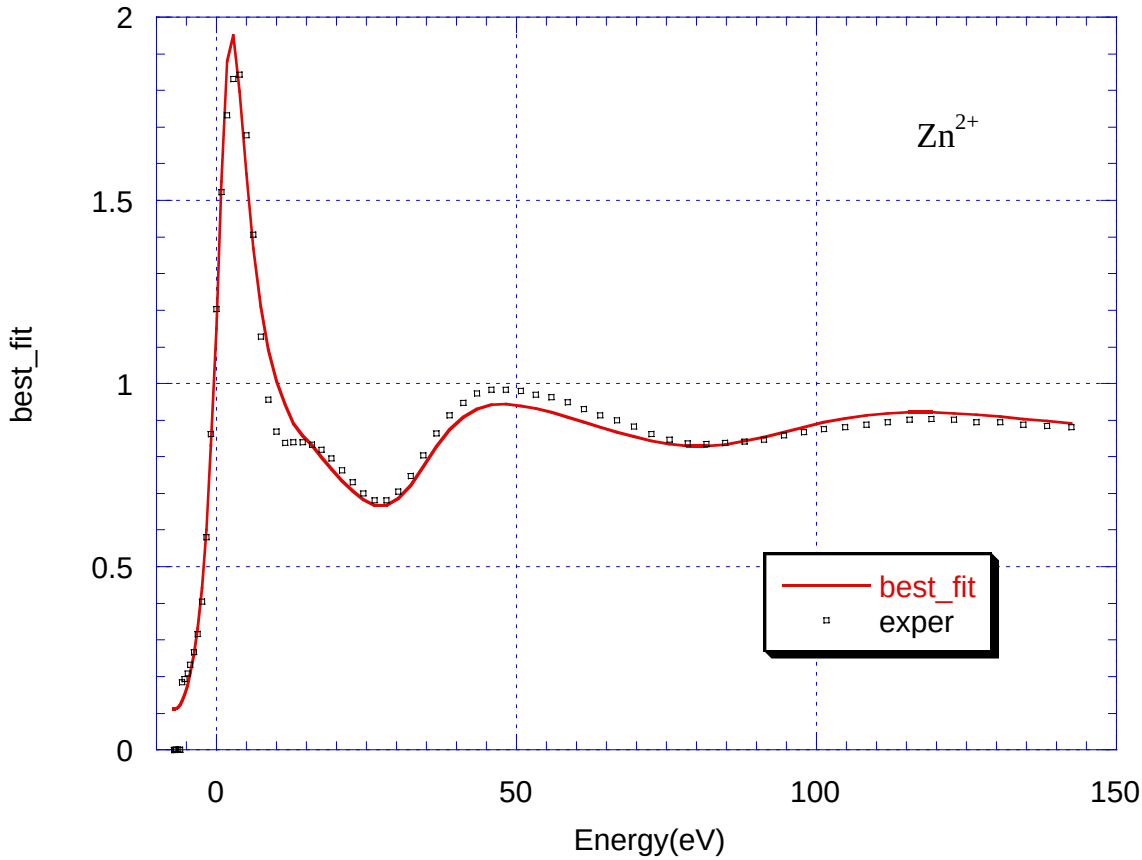

Octahedron with a Zn-O distance = 2.05±0.05 Å

R_{sq} = 4.77

The agreement between exp. and b.f. calculation decrease but the structural result remains stable.

Zn^{2+} - Effects of cluster deformation

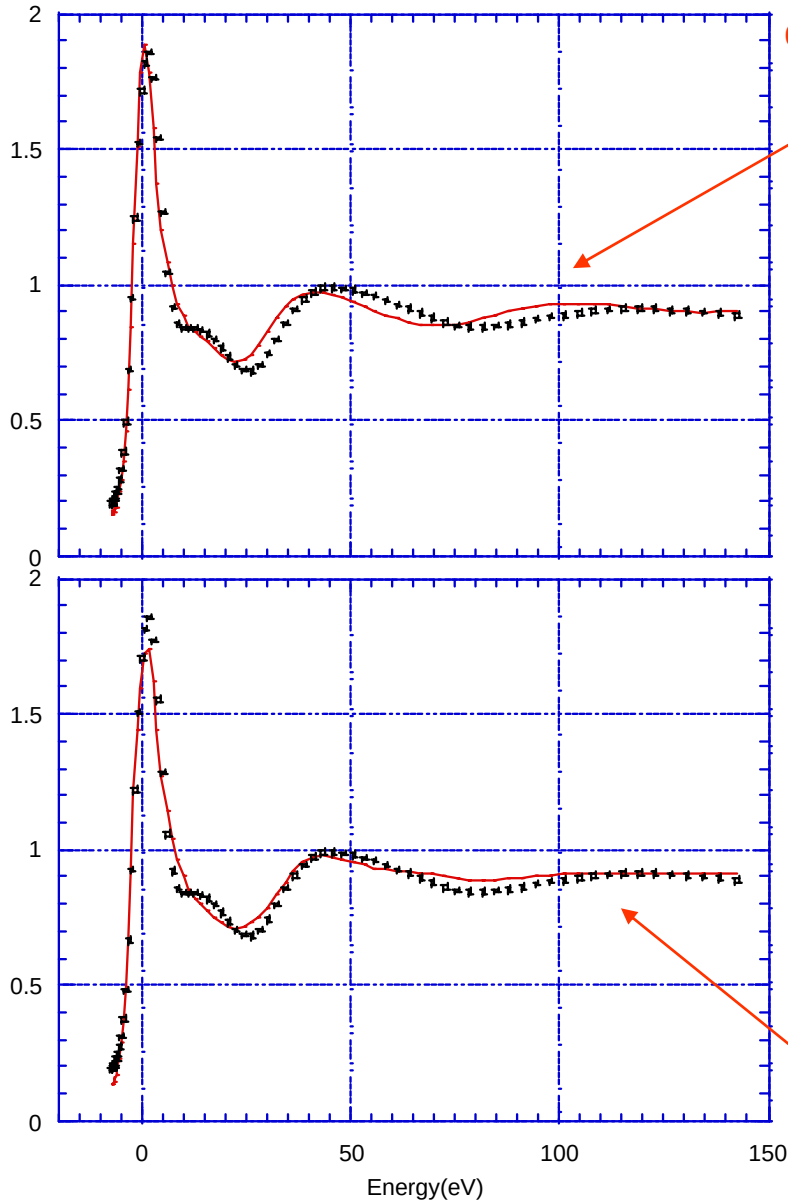

Increase of Zn-O distance up to 2.16 Å

R_{sq}=6.0

R_{sq}=4.2

J.T. distortion of the axial oxygen atoms of 0.2 Å

Geometrical effects are bigger than potential effects

$Fe(CN)_6$

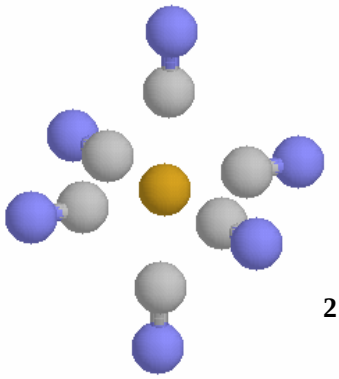

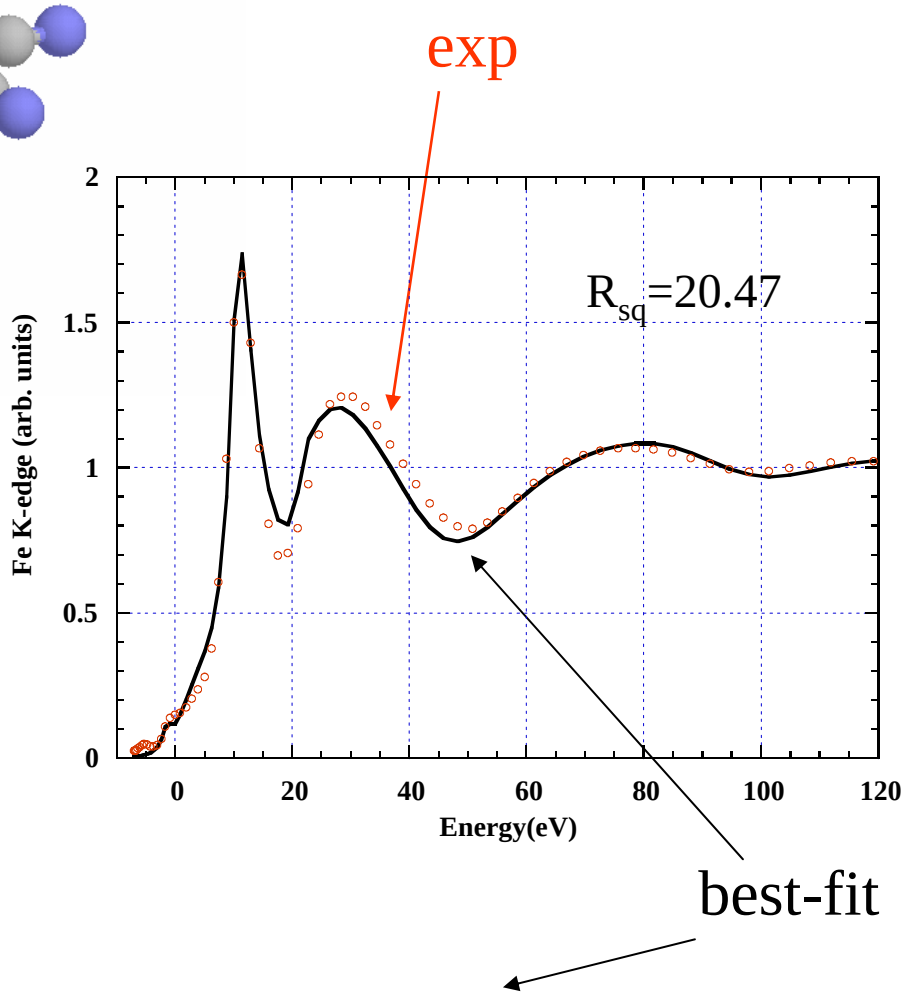

The best-fit condition corresponds to an octahedral symmetry with Fe-C distance of 1.93(0.01) Å and C-N distance of 1.15(0.01) Å

Previous GNXAS analysis (Westre et al. JACS 117 (1995)) reports Fe-C and Fe-N distances of 1.92 Å and 1.18 Å respectively

Fit with NO molecules
Fe-N =1.91Å and N-O =1.16Å

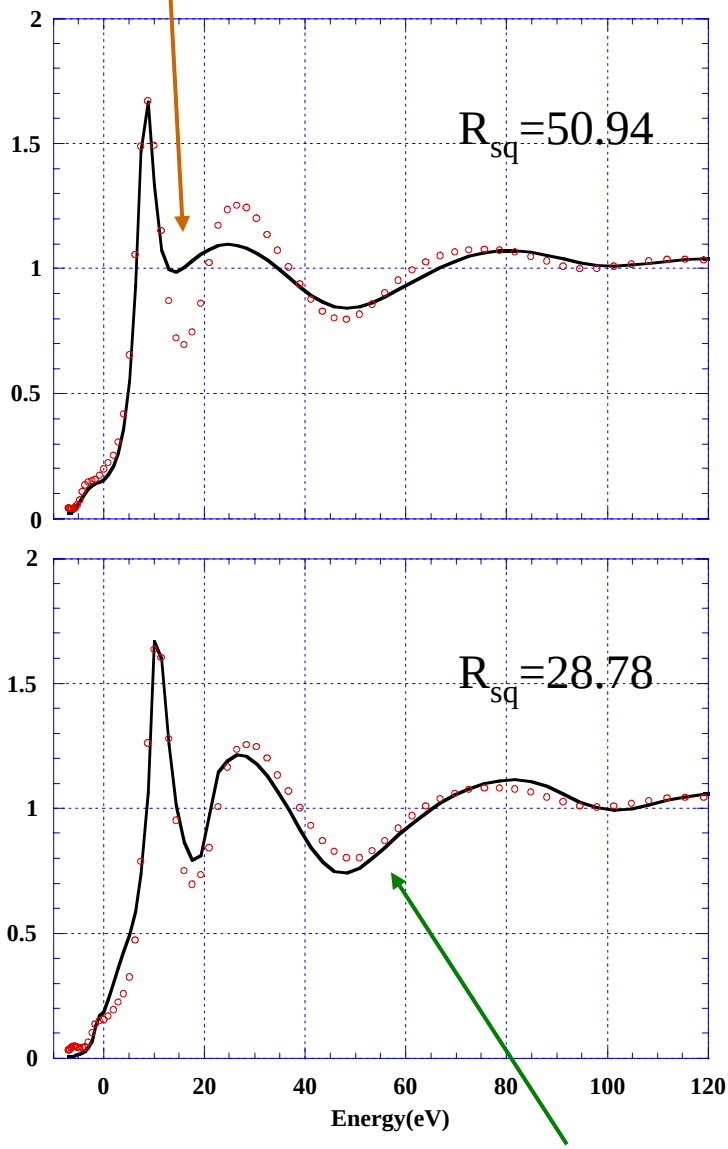

Fit with CO molecules
Fe-C =1.94Å and C-O =1.11Å

•Hexakis(imidazole) Cu(2+)Nitrate

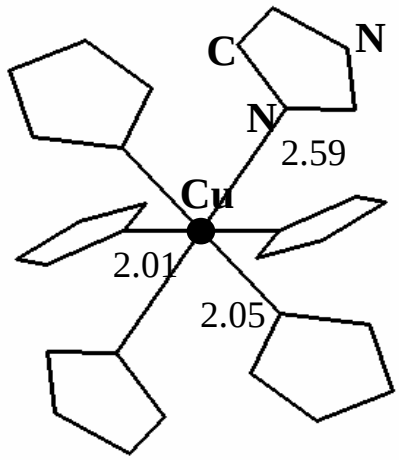

Starting ***Sq.Res.:73.4***

R_1=2.31 R_2=2.35 R_3=2.39

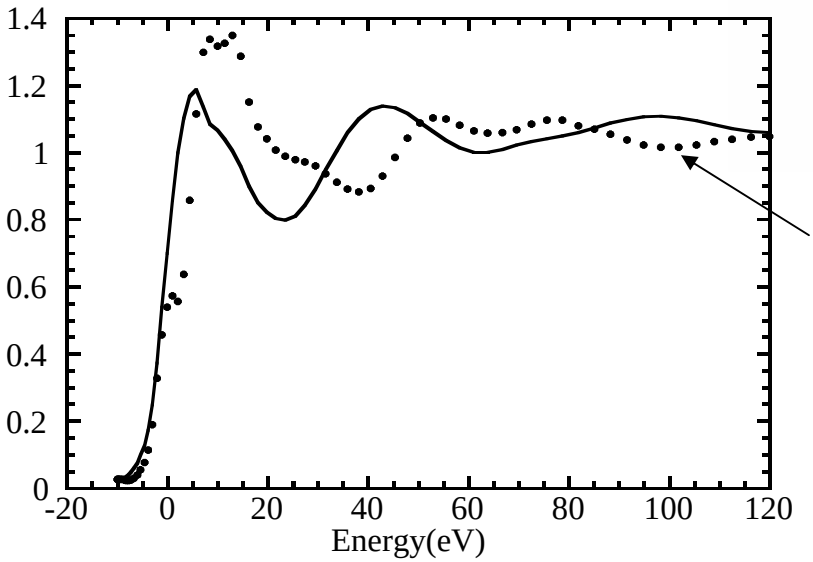

exp

Best fit ***Sq.Res.: 5.4***

R_1=2.04(3) R_2=2.05(4)

R_3=2.59(9)

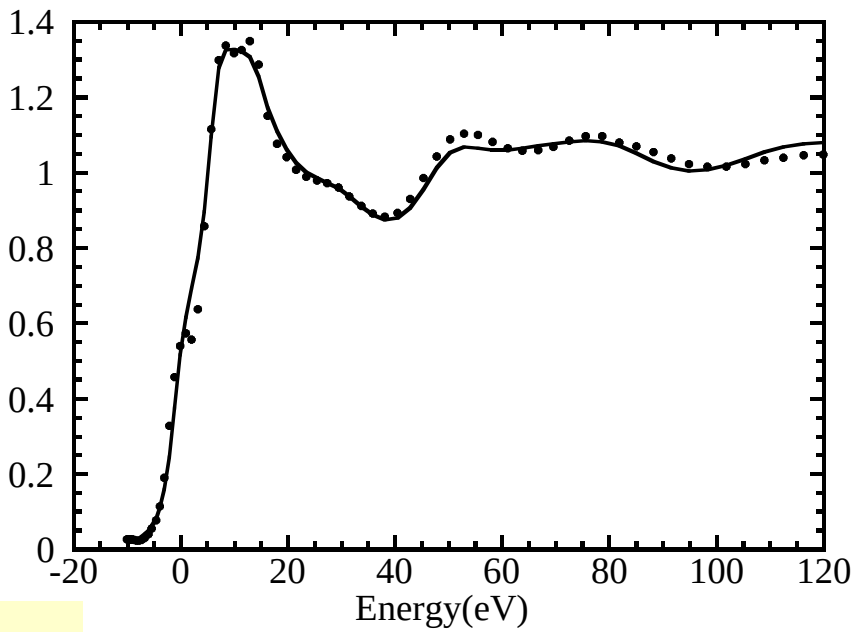

Consistent with XRD data within 0.03 Å

Coordination geometry of Cu^{2+} in solution

- Fivefold or sixfold coordination?

- J.T. distortion?

Car – Parrinello molecular dynamics calculation
A. Pasquarello et al. Science (2001)

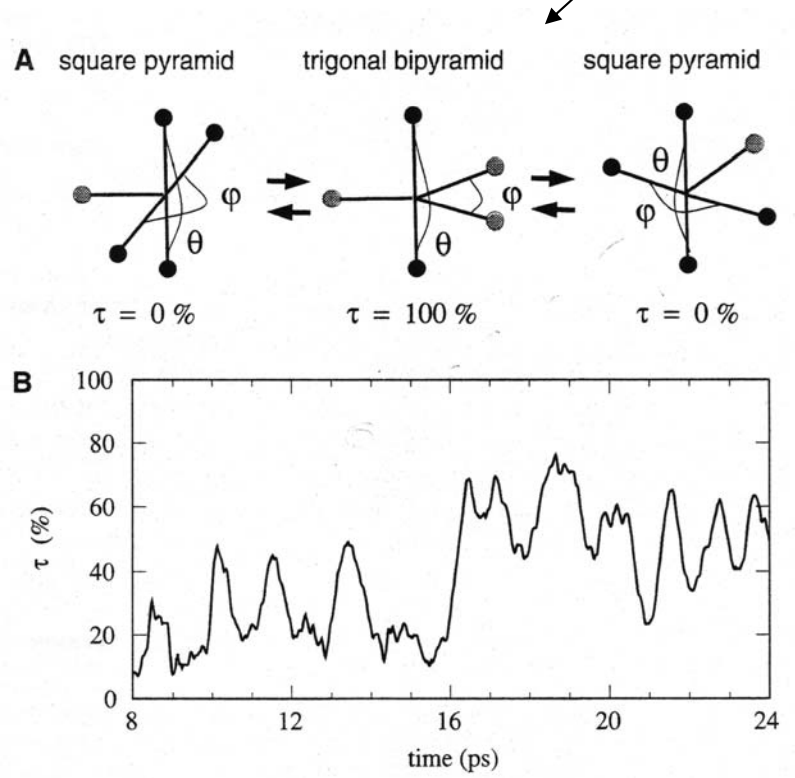

GNXAS analysis

0.1 M Cu^{2+} water solution
H atoms are included

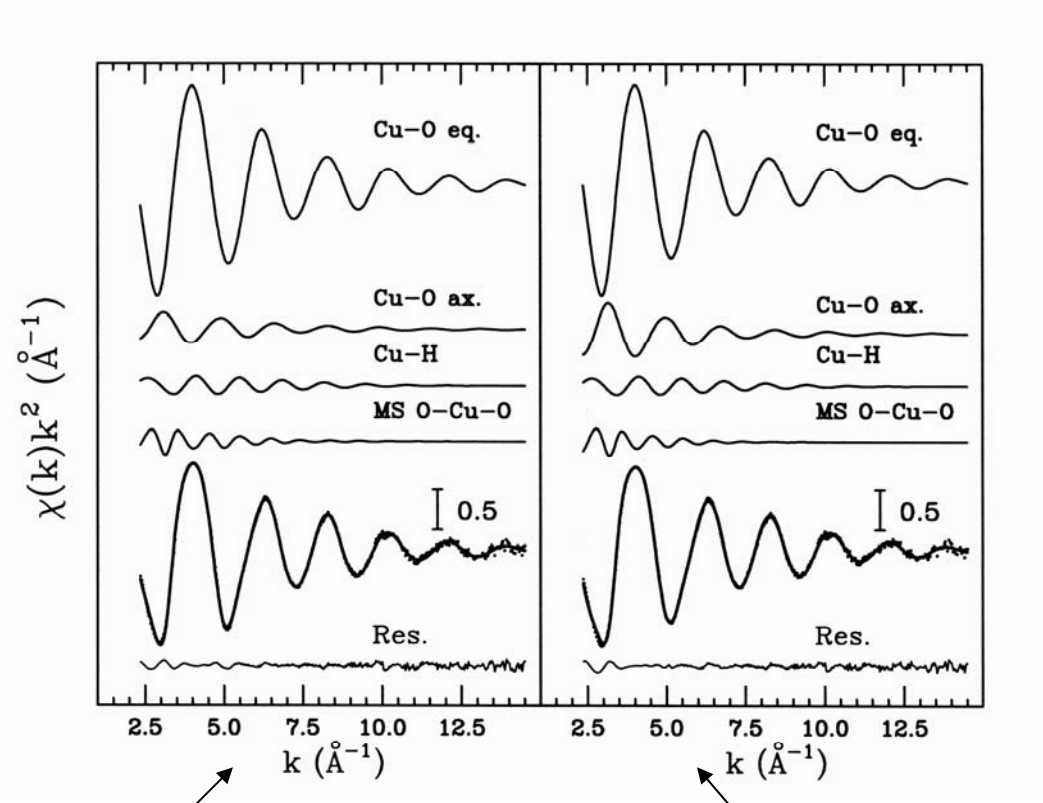

Fivefold coordination

sixfold coordination

Two geometries with the same accuracy

4 equa. O at 1.96 Angs
1 axial O at 2.36 Angs

4 equa. O at 1.96 Angs
2 axial O at 2.36 Angs

MXAN analysis

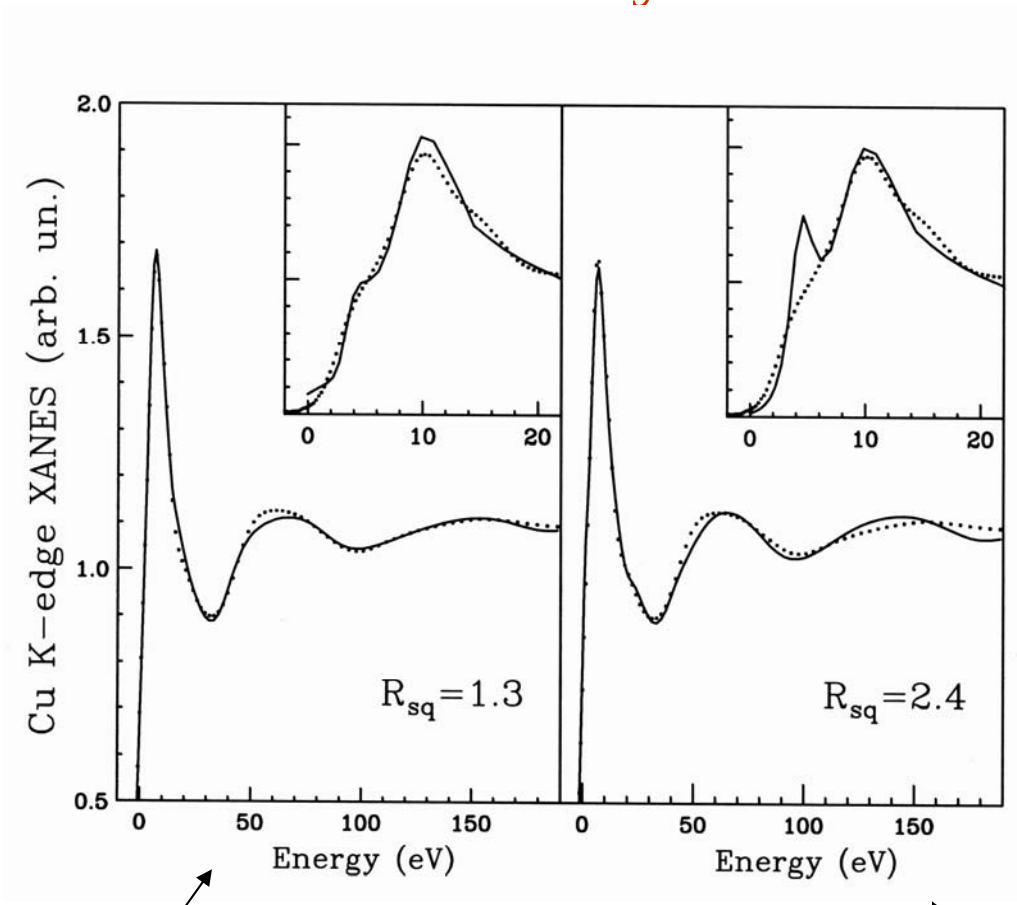

Fivefold coordination

sixfold coordination

Two different solutions

4 equa. O at 1.97(1) Angs
1 axial O at 2.39(6) Angs

4 equa. O at 1.99(1) Angs
2 axial O at 2.56(4) Angs

Combining the two possible solutions

An average fivefold coordination geometry

	N	R	σ^2
Cu-$O_{eq.}$	4	1.956(4)	0.0053(5)
Cu-$O_{ax.}$	1	2.36(2)	0.010(3)

A possible dynamic picture

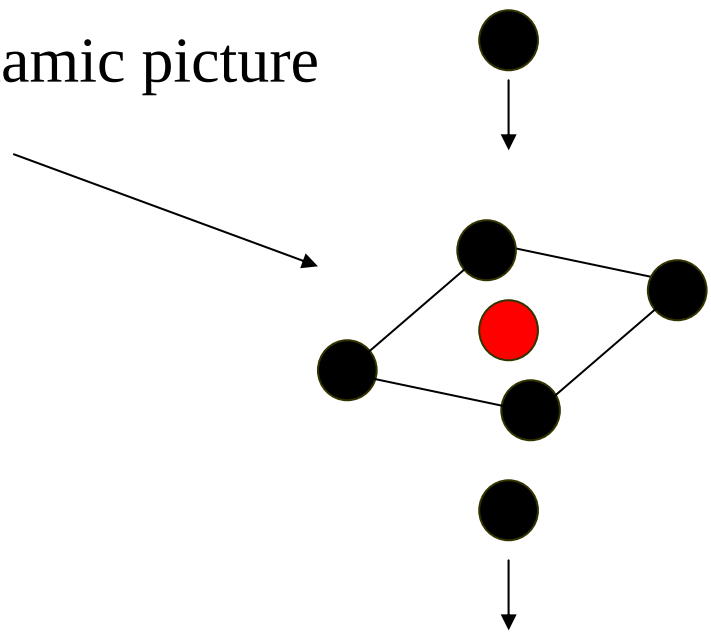

Comparison with neutron diffraction

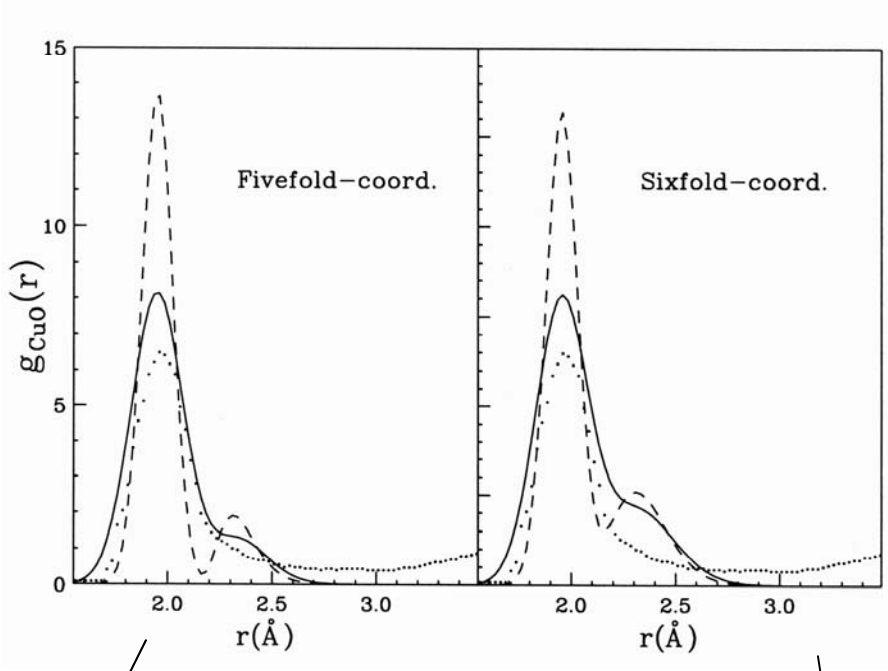

	N	R	σ^2
Cu-$O_{eq.}$	4	1.956(4)	0.0053(5)
Cu-$O_{ax.}$	1	2.36(2)	0.010(3)

	N	R	σ^2
Cu-$O_{eq.}$	4	1.961(4)	0.0058(5)
Cu-$O_{ax.}$	2	2.36(2)	0.020(3)

Sperm whale myoglobin single crystal

Space group $P2_1$

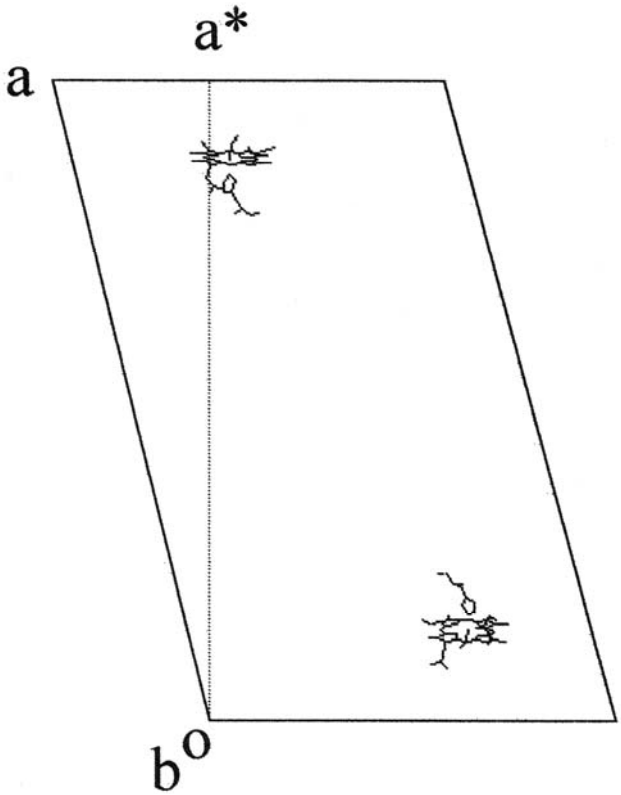

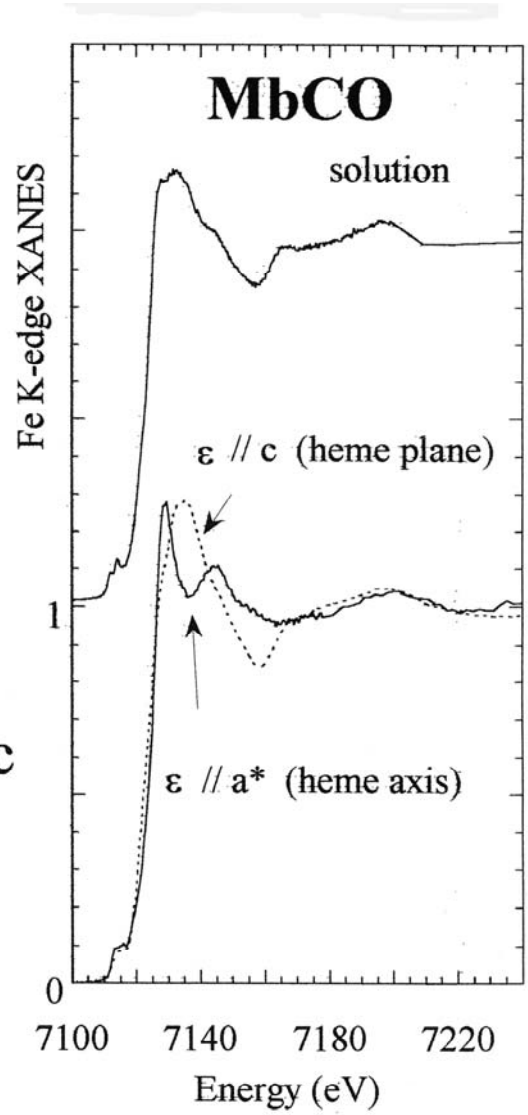

Unit cell data

a = 64.18 Å

b = 30.84 Å

c = 34.69 Å

P-XANES of MbCO and Mb*CO

Experiment by S. Della Longa et al. J. Synchr. Rad. **6**, 1138 (1999)

MbCO

Mb*CO

Small MbCO
single crystal
0.2*0.2*0.3 mm

BM32 at ESRF
- X-ray dynamic focusing
- 30 elem. fluorescence
  X-ray detetector

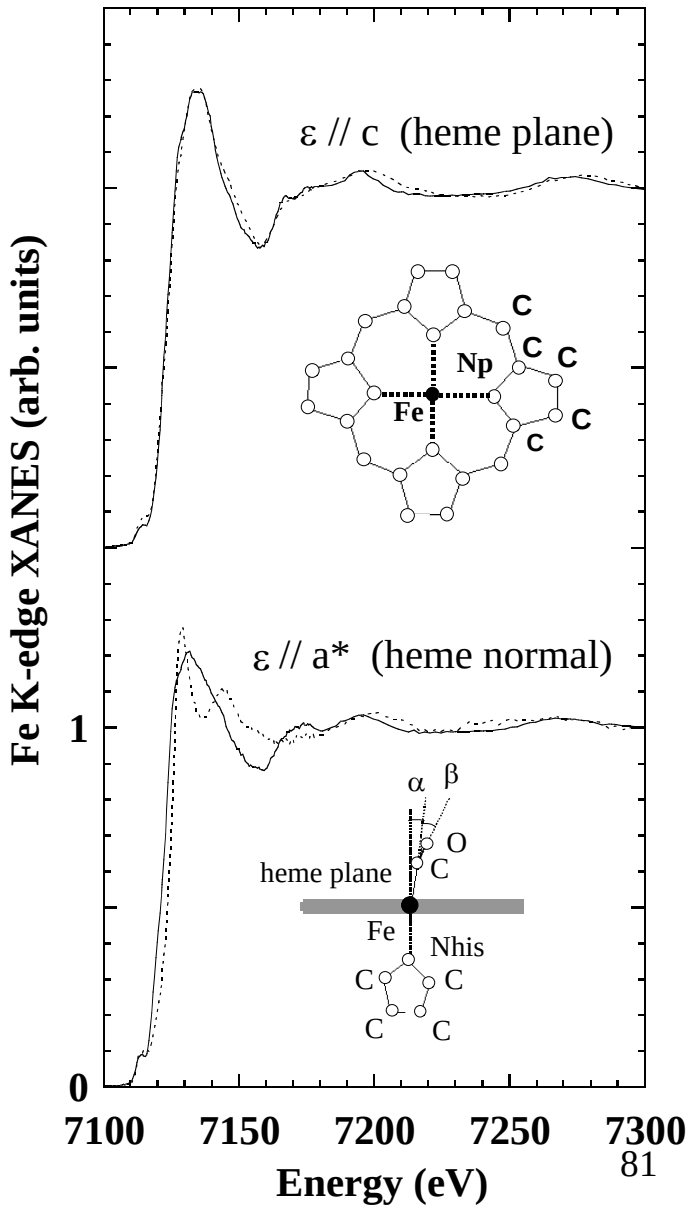

XANES quantitative analysis of MbCO and Mb*CO

S. Della Longa, A. Arcovito, M. Girasole, J.L. Hazemann and M. Benfatto, Phys. Rev. Lett. **87**, 155501 (2001)

cluster of 32 atoms

l_{max} and cluster size on the basis of convergence criterion

MT radii according Norman criterion

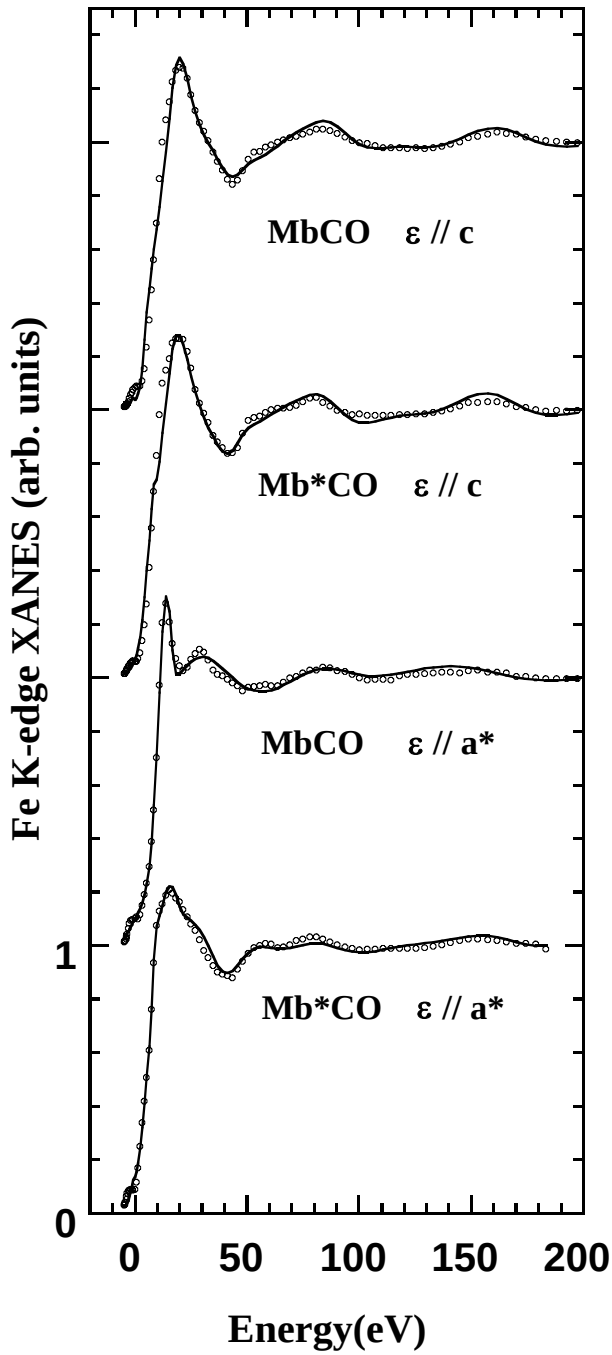

Fitted results

MbCO

Exp.	Fe – Np	Fe – Nhis	Fe – C	α	β	C – O
XRD (1) ***1.5Å***	1.97	2.19	1.92	3	38	1.17
XRD(2) ***1.1Å***	1.98	2.06	1.73	4	7	1.12
XRD(3) ***1.1Å***	1.98	2.06	1.82	9	9	1.09
EXAFS(4)	2.01	2.20	1.93	--	--	--
XANES	2.00(2)	2.06(3)	1.83(2)	--	14(4)	1.07

(1) PDB code: 1MBC; (2) PDB code: 1BZR; (3) PDB code: 1A6G;
(4) Powers et al. - solution

High XANES sensitivity to the CO position

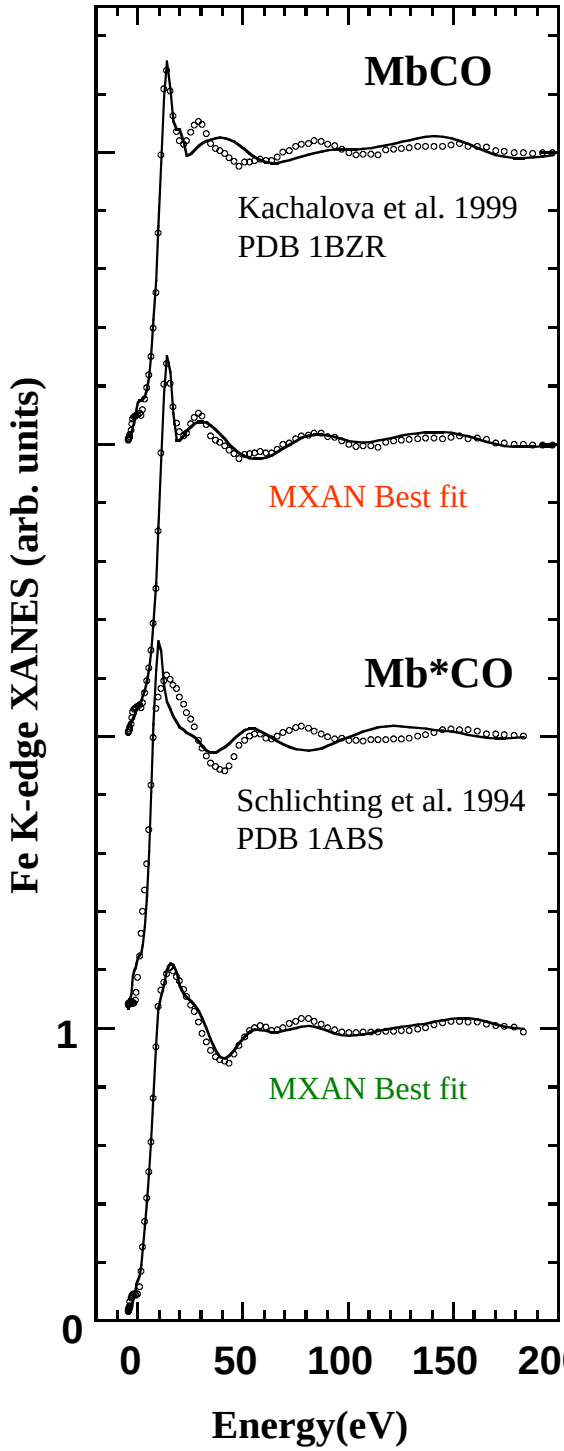

MXAN analysis on hemoproteins in solution

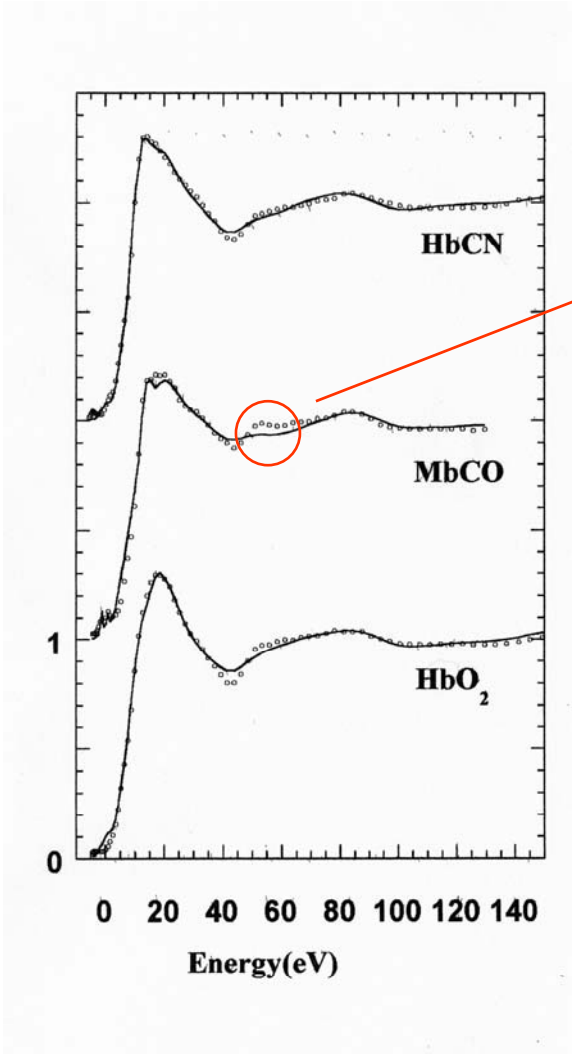

Presence of some discrepancies

sample	Fe-Nhis	Fe-ligand	β	L_1-L_2 bond
HbO2	2.18(4)	2.02(2)	65(12)	1.31
MbCO cry	2.06(3)	1.83(2)	14(4)	1.07
MbCO sol.	2.02(4)	1.72(4)	6(4)	1.11
HbCN	2.22(7)	2.03(5)	<30	1.05

Some conclusions

- **It is possible to make fit in the XANES energy range starting from the edge by a full MS approach**

- **The geometrical structure dominates the XAS spectroscopy**

- **Many applications** { **Biology**, **Impurity**, **.....**